MEASUREMENTS AND THEORETICAL INTERPRETATION OF HALL CURRENTS FOR STEADY AXIAL DISCHARGES IN RADIAL MAGNETIC FIELDS

By Philip Brockman, Robert V. Hess,
and Richard Weinstein [1963] 42p 16 refs

NASA Langley Research Center
Langley Station, Hampton, Va.

Presented at the ~~Fifth~~ 5th Biennial ~~G~~as Dyn~~amic~~s Symp~~osium~~

Evanston, Illinois
Aug~~ust~~ 14-16, 1963

MEASUREMENTS AND THEORETICAL INTERPRETATION OF HALL CURRENTS FOR STEADY AXIAL DISCHARGES IN RADIAL MAGNETIC FIELDS[1]

Philip Brockman,* Robert V. Hess,*
and Richard Weinstein*

NASA Langley Research Center
Langley Station, Hampton, Va.

SUMMARY

15616

Experiments for Hall-ion accelerator are presented using axial electric fields and radial magnetic fields. Measurements of the variation of Hall currents with magnetic field for various constant axial currents are presented together with voltage variations. The pressures in the experiments vary from 6 to 40 μ Hg, the magnetic fields from 0 to 500 gauss, and the currents from 1 to 40 amperes. The Hall currents first increase with magnetic field and then decrease again as the magnetic field is increased. The variation can be interpreted in terms of Joule- and ion-slip losses for the partially ionized plasma used in the experiments. The effect of transition to turbulence is also evaluated and the present state of the theory for turbulent conduction is discussed. Preliminary experiments for preionization and for the heating of ring-shaped cathodes to thermionic emission are discussed.

INTRODUCTION

The research on acceleration of plasmas or ions in plasmas using azimuthal Hall currents and radial magnetic-field components has grown considerably since early work on Hall current plasma accelerators at the NASA Langley Research Center (ref. 1) and subsequent description of an added ion acceleration mechanism for improvement of a traveling wave accelerator by AVCO Everett Research Laboratory (ref. 2). The final grouping of the latter mechanism of ion acceleration under the principle of Hall-ion acceleration is based on the efforts of many research laboratories; Electro-Optics, General Electric, the Lewis and Langley Research Centers of NASA, and United Aircraft. A history of the development of Hall current accelerators is given in reference 3 in the section "Acceleration Using Hall

---

[1]Part of the material in this paper has been presented by Mr. Brockman as a thesis in partial fulfillment of the requirements for the Degree of Master of Arts at the College of William and Mary.

*Aerospace Engineer.

Currents." The reason for the interest in Hall current accelerators is that they offer the possibility of magnetic containment, increased uniformity of discharges, reduction in electrode erosion, and operation over a very wide range of density and specific impulse.

There are several reasons for measuring Hall currents. One, more or less obvious one, is that it gives an independent check of the thrust, which can be compared with direct thrust measurements. In this connection it should be noted that the total voltage drop must overcome the losses as well as accelerate the ions, so that this voltage drop is only a true measure of the electrostatic force on the ions if the losses are small.

The present measurements of Hall currents differ from those previously performed at the Langley Research Laboratory (refs. 4 and 5) in that a much greater number of measurements were made at various axial currents and magnetic fields. By cross-plotting the results to indicate variation of Hall currents with magnetic field at a variety of constant axial currents, it was possible to establish more definite trends which were only suggested by the experiments in reference 5. Simultaneous measurements of the variation of axial voltage drop with magnetic field were also performed. In the present experiments measurements were also made over a wide current range for considerably lower pressures than previously reported by us. A special effort has been made to evaluate up to what point the novel effects can be interpreted through conventional loss mechanisms rather than through the popular field of plasma turbulence.

Finally, it should be pointed out that the Hall current apparently can provide vital information on certain anomalous or "turbulent" conduction effects which have recently received considerable attention. In the first study (to the writer's knowledge) of instabilities and turbulent conduction effects in a Hall current accelerator which was conducted at the Langley Research Center (ref. 6), probes which were placed in the azimuthal direction of the Hall current indicated that although coaxial symmetry was imposed by the electrodes and the magnetic-field distribution, the plasma did not maintain symmetry under all conditions. At the same meeting Dr. Buneman independently emphasized in the Round Table Discussion the importance of checking for plasma asymmetrics in geometrically symmetric experimental arrangements. The azimuthal Hall current could be especially sensitive to deviations from symmetry and thus could offer a clue to the transition from conventional to turbulent conduction. Preliminary application of these concepts to the Hall-ion accelerator are discussed in the preprint with more details to be presented in the talk.

Experiments for the preionizer and the thermionically heated cathodes have up to date been made in a separate test apparatus. The preionizer was designed and operated by J. Burlock and T. Collier and the heated cathode by O. Jarret. Details are given in appendixes B and C.

An experimental study of the influence of preionizers and heated cathodes on Hall currents, electric fields, and oscillations is being undertaken.

The major purpose of this paper is to gain an understanding of the acceleration mechanisms in a low-pressure Hall current accelerator. From a more

fundamental viewpoint it is the aim to obtain an understanding of the mechanism of electric conduction across a magnetic field in the presence of ion motion.

Hall currents also have been measured for a high-power high-pressure plasma Hall accelerator and a Hall-ion accelerator operating in this range also has been constructed (see also studies at Electro-Optics, ref. 7). Results of these experiments will be reported at a later date.

The research was performed in the Plasma Physics Section of the Magneto-plasmadynamics Branch.

SYMBOLS

$\vec{B}$	magnetic flux density
$\bar{c}$	mean thermal velocity
e	charge on singly ionized ion
$\vec{E}$	electric field strength
$\vec{E'}$	$\vec{E'} = \vec{E} + \vec{v}\times\vec{B}$
$\vec{j}$	current density
l	length
m_e, m_i	mass of electron and ion
m	meter
n	particle density
p	pressure
Q	collision cross section
r_L	Larmor radius
t	time
T	temperature
$\vec{v}$	center of mass velocity
V	voltage
W	$W = \dfrac{(1 + 2\omega_e\tau_e\omega_i\tau_i)}{\omega_e\tau_e}$

α quantity defined in equation (13)

λ mean free path

μ microns

ν collision frequency

σ_o conductivity in the absence of a magnetic field, $\sigma_o = \frac{n_e e^2 \tau_e}{m_e}$

τ mean free time between particle collisions

ω_e, ω_i cyclotron frequency $\omega_e = \frac{eB}{m_e}$, $\omega_i = \frac{eB}{m_i}$

Subscripts:

e electron

i ion

n neutral

r,θ,x refer to cylindrical coordinate system

Superscript:

$\overrightarrow{( )}$ vector quantity

APPARATUS

A schematic of the apparatus is given in figure 1. The electrodes are 7.3 cm I.D. inserts within water-cooled holders. The inserts are copper at the anode and aluminum at the cathode in the experiments reported here, but these may be easily replaced by any other material. The edges of the electrodes and the glass are protected from the discharge by boron nitride insulators; these insulators leave 2.54 cm of the electrodes exposed to the discharge. The center glass is 7.3 cm I.D. and the discharge length 22.86 cm. On either side of the discharge the electrode holders are connected to glass crosses. These crosses contain Hasting thermocouple vacuum gages. The anode cross is connected to the gas input and the cathode cross leads to the vacuum system. The cathode cross also contains a cantilever support for a bakelite rod which, in turn, supports an iron bar in the center of the discharge. The iron bar is centered under the magnet and is 22.9 cm long, the bar is 3.16 cm O.D. and has a 1.27-cm hole through the center. This hole contains a teflon rod which is screwed to a boron nitrode insulator at the anode end and to the bakelite rod at the cathode end.

The iron bar is covered by a 38-cm pyrex tube. This cantilever arrangement was designed so that the accelerator can be mated with any type of preionizer at the anode and without changing the configuration or interfering with the flow from the preionizer. The magnet solenoid is 2.8 cm long and its center is 10.16 cm from the anode and 12.7 cm from the cathode. It is a 450-turn coil and is powered by ten 6-volt batteries; it is current controlled by means of a variable resistor. A search coil is mounted $4\frac{1}{2}$ cm from the center of the magnet on the cathode side. This is a 100-turn coil and it is connected in series with a ballistic galvanometer. The arc power supply is a 700-volt 1,400-ampere motor-generator set and is connected to the electrodes through a 10.37-ohm ballast resistor. The pumping system consists of a cold trap, a 14-inch diffusion pump, and a Stokes vacuum pump. Figure 2 is a diagram of the magnetic field configuration for an average radial field of 100 gauss - a rapid increase of axial field strength occurs above 500 gauss due to saturation of the iron bar.

The investigations reported here are a study of the basic mechanisms of the discharge. The pumping system at this time is not adequate to remove the mass flow due to high ion currents. As a consequence, during operation there is a pressure rise at the pump entrance and a pressure drop at the gas inlet. This results in a flow of neutral particles from cathode to anode. The back flow or circulation of neutrals permits the maintenance of high ion currents. A larger vacuum system (four 35-inch diffusion pumps) is now under construction, to be used for experiments at high specific impulse.

OPERATION OF DISCHARGE AND MEASUREMENTS

As the solenoid is in the center of the discharge, the radial magnetic field reverses direction from the anode to the cathode side of the discharge. This will also reverse the direction of the Hall current and of any gas rotation as these are functions of $\vec{V} \times \vec{B}$. However, the forces will remain in the same direction as these are functions of $(\vec{V} \times \vec{B}) \times \vec{B}$. Thus, the reversing magnetic field has the advantage of tending to destroy any gas rotation which may build up on one side of the magnet. On the cathode side of the discharge the gas will enter with any rotation that has built up; on the anode side the rotating force will then be reversed and the average rotation on the cathode side should be close to zero.

The discharge for these experiments was operated with no preionizer. Thus, all ionization was supplied by the electric field. Starting ionization was supplied by a Telsa coil, but this was turned off before any measurements were taken. Voltage and current were monitored on standard meters and also recorded on a Consolidated Electric Co. oscillograph. Pressure was monitored on two Hastings thermocouple gages and also recorded on the Consolidated instrument. Hall current was measured by means of a 100-turn search coil and ballistic galvanometer. The discharge was turned off and the collapsing magnetic field of the Hall current induced an e.m.f. in the search coil. The search coil was connected in series to the ballistic galvanometer through a 15-ohm resistance; the current through this circuit was integrated by the ballistic galvanometer giving the

total charge. This charge is proportional to the original Hall current. The ballistic galvanometer was calibrated by placing two 80-turn coils in place of the Hall current. These coils were 5.3 cm in diameter and 7 cm in length. The ballistic galvanometer was calibrated by running various currents through the coils. The direction of current was reversed in the two coils to represent the Hall current. When the current was turned off, the reading on the galvanometer was taken. The calibration was retaken at several magnetic field strengths in order to check if any saturation of the iron bar was affecting the readings. A slight drop in reading was noted at 550 gauss but this drop was within reading error. However, the sudden increase of the axial field at saturation may explain the sharp dropoff in Hall current. This effect is negligible below 550 gauss. The ballistic galvanometer was calibrated in amperes and the area of the Hall current was estimated at 17.79 cm^2. According to visual observation the discharge area did not vary much above a magnetic field of ~10 gauss. The current was multiplied by $10^4/17.79$ to give amperes per square meter. The axial current was multiplied by $10^4/30.59$ to give amperes/m^2 and the arc voltage multiplied by 100/22.86 to give volts per meter. Mass flow was measured by a tri-flat flow tube and a standard pressure meter. Magnetic field was calibrated vs. current in magnet by a gauss meter. Magnet current was set with a standard ammeter.

In operating the discharge pressure was set using a variable leak; the voltage across the electrodes and the magnetic field were preset. The discharge was started with the Tesla coil and when voltage and current oscillations as observed on the meters had settled out, the oscillograph was started and the switch controlling the ballistic galvanometer was depressed. The discharge was then turned off and the reading on the ballistic galvanometer taken by hand. Ideal operation would have been to operate the discharge at constant current for various magnetic-field strengths. However, as the power supply was not current controlled it was difficult and time consuming to adjust the current during each run. At each magnetic-field strength the discharge was started at various voltages; the running voltage and current were allowed to adjust themselves. After preliminary data reduction more data were taken in regions of interest. In order to extend the range of currents at high magnetic-field strengths, it was sometimes necessary to start the discharge and then adjust the voltage downward. Data were taken at 15, 30, and 40 microns and these data are presented in the form of arc voltage in volts/meter and Hall current in amperes/m^2 plotted vs. arc current in amperes/$meter^2$ for various magnetic-field strengths.

The data were then cross-plotted to give arc voltage and Hall current vs. magnetic-field strength for various arc currents. These curves are presented in figures 3 to 6.

The primary purpose of this study was to measure the Hall currents. Making a survey of any parameter is time consuming and thus several measurements which are needed for a complete analysis have not yet been made. A program has been active for some time to measure local voltage drop with floating probes and to make some measurements of ion density and electron temperature with Langmuir probes and double probes. The floating probe errors should cancel if the probes are close together so that the plasma conditions are equal at both probes. However, the

magnetic field will influence the electron temperature and ion density measurements to some extent (ref. 8). The variation of these parameters should be comparable at any constant magnetic-field strength, but there is some question in comparing measurements taken at different magnetic-field strengths. An attempt will also be made to measure velocities and forces in the accelerator.

A few basic measurements of oscillations in the discharge have been made with a simple metal plate capacitively coupled to the discharge through the glass. A survey of oscillations with probes placed in the plasma will be reported in the talk.

INTERPRETATION OF RESULTS

The most striking result found is the increase, peaking, and decrease of Hall current with increase of magnetic field at constant axial current. The initial increase of the Hall current with increasing axial current at constant magnetic field and the form of the arc voltage versus axial current curves at constant magnetic field has been previously reported (ref. 4). The shape of the curves of arc voltage versus magnetic-field strength are different in certain regions than those normally reported (e.g., refs. 9 and 10), but this may be due to the inherent errors in measuring total arc voltage rather than local electric field, or it may be due simply to our particular operating condition.

Since the experiments are concerned with a partially ionized plasma in a magnetic field and include the motion of ions with respect to neutrals, it is of interest to see to what extent the experiments can be interpreted in terms of the conventional generalized Ohm's law including ion slip. The influence of turbulence is discussed in a later section.

Repeating equation (A4) from appendix A, which is the complete equation for j_θ including motion of ions and neutrals but not turbulence,

$$-j_\theta = \frac{1}{W}\left(j_x - n_e e v_x\right) \tag{1}$$

The inclusion of $2\omega_i\tau_i\omega_e\tau_e$ in the term

$$W = \frac{1 + 2\omega_e\tau_e\omega_i\tau_i}{\omega_e\tau_e}$$

gives the influence of ion slip. The ion slip term will increase W and, therefore, decrease j_θ at constant magnetic field. However, solving equation (A2) for E_x'

$$E_x' = \frac{1 + W^2}{W} \frac{j_x B}{n_e e} - \frac{v_x B}{W} \tag{2}$$

The effect of ion slip on E_x' is more complicated than on j_θ. The term

$$\frac{1 + W^2}{W} = \frac{1}{W} + W = \frac{\omega_e \tau_e}{1 + 2\omega_e \tau_e \omega_i \tau_i} + \frac{1 + 2\omega_e \tau_e \omega_i \tau_i}{\omega_e \tau_e} \tag{3}$$

Thus for $W \ll 1$ an increase in $\omega_i \tau_i$ will decrease E_x' (through increase in ion current) but for $W \gg 1$ an increase in $\omega_i \tau_i$ will increase E_x' (neglecting v_θ). For constant j_x the increase then decrease of $-j_\theta$ is due either to variations of W or v_x or n_e with B. At the particular conditions that we operate n_e is probably small and v_x the average (or center of mass) plasma velocity is limited, as pointed out in the section on apparatus. It, therefore, seems that the effect of $n_e e v_x$ can be neglected, for the present case.

A simple explanation of the variation of Hall current with magnetic field can be based on the variation of W with magnetic field. The following assumptions were made: first, that $n_e e v_x$ was negligible compared to j_x, and, second, that τ_e and τ_i were constant for j_x constant. This second assumption is based on the condition that τ_e and τ_i are not explicit functions of E_x' or B. The calculated values of $\omega_e \tau_e / B$ and $\omega_i \tau_i / B$ in the literature usually depend on equivality of electron and ion temperatures - we know that our low-pressure operation does not justify this assumption. In order to generate some theoretical curves for j_θ vs. B, equation (1) is rewritten in the form

$$W = \frac{j_x}{-j_\theta} \tag{4}$$

and then for a particular experimental curve a calculation is made of the minimum value of W, as $W_{min} = \frac{j_x}{-j_{\theta,max}}$. The values of $\frac{\omega_e \tau_e}{B}$ and $\frac{\omega_i \tau_i}{B}$ were then calculated for this case using equations (A11) and (A12).

These values were then divided by the magnetic-field strength at the maximum j_θ point. The resultant values of $\omega_e \tau_e$ and $\omega_i \tau_i$ were used with equation (A7) to calculate W as a function of B. Typical plots of $1/W$ vs. B and $(1 + W^2)/W$ are given in figure 7. Equation (4) was then used to calculate theoretical values of j_θ vs. B. Equation (2) was used to calculate values of $n_e e E_x'$ vs. B. The sheath voltage was assumed to be equal to the experimental voltage at $B = 0$ and it was also assumed that n_e was constant; for constant j_x a value of n_e was chosen so that the highest point of the experimental and

theoretical E_x' vs. B curves would match and the assumed sheath voltage was added to the theoretical curves so that the bottom points would also match. Thus, only the shape of these curves can be compared. The method of calculating the W_{min}, of course, forces the experimental and theoretical Hall current curves to match at $j_{\theta,max}$. In figure 8 experimental and theoretical curves of j_θ vs. B are compared for j_x = 3,930, 5,240, and 9,170 amp/meter^2; at j_x = 3,930 amp/m^2, W_{min} = 0.2, B = 0.015 web/meter^2, $\omega_e\tau_e/B$ = 668, $\omega_i\tau_i/B$ = 3.32; at j_x = 5,240, W_{min} = 0.1158, B = 0.015 web/meter^2, $\omega_e\tau_e/B$ = 772, $\omega_i\tau_i/B$ = 2.9; at j_x = 9,170, W_{min} = 0.1274, B = 0.0125, $\omega_e\tau_e/B$ = 1,256, $\omega_i\tau_i/B$ = 2.55. In figure 9 the theoretical and experimental curves of E_x' vs. B are compared for j_x = 5,240 at 30 microns Hg. 247 volts/m have been added to the theoretical curve to account for sheath voltage at B = 0; for curve matching n_e was adjusted to be 2.67×10^{18} particles/m^3. This corresponds to a very reasonable few percent ionization. The values of $\omega_i\tau_i/B$ and $\omega_e\tau_e/B$ show also reasonable agreement with theory (ref. 7) especially if the excess of electron temperature is considered. The Hall current curves match quite well and seem off by only a slight rotation. This can be due to the error involved in neglecting various effects when calculating W_{min}. The E_x' curve does not match as well except at the low- and high-magnetic-field strengths where the general curvature is the same.

In matching theory with experiments, one must also be reminded that the values for E_x' in figures 5 to 6 are based on averaging the voltage drop over the length of the apparatus including sheath drop. Only isolated measurements have been made so far of the voltage distribution in the accelerator. A complete survey is, however, necessary to obtain a more detailed account of the contribution in sheath drop with varying magnetic field. One should also be reminded that the electric field appearing in the equations is given by $E_x' = E_x - v_\theta B$ where E_x is the measured quantity.

Although special care has been taken to reverse B in the acceleration process, a certain amount of rotation will exist. The effect of rotation can also reduce j_θ/j_x but it appears unlikely that it would be the sole effect since the drop in j_θ begins at values of $\omega_i\tau_i$ $\left(\text{which approximately equals } \lambda_i/r_{Li}\right)$ considerably below unity. Preliminary observations of the rotational speed of the discharge also indicate that it is low.

Before it can be stated with assurance that ion slip is the main contributor and not turbulence (see next section), several additional measurements are necessary. These include measurements of n_e, v_x, local measurements of E_x, and measurements of turbulent effects. Also, measurements of electron and gas temperatures would be helpful in calculating directly values of τ_e and τ_i.

COMPARISON WITH OTHER THEORETICAL APPROACHES

Neglect of Ion Slip and Loss-Free Case

For negligible values of $\omega_e\tau_e\omega_i\tau_i$, the ion-slip losses can be neglected and equation (A4) in appendix A changes from

$$-j_\theta = \frac{\omega_e\tau_e}{1 + 2\omega_e\tau_e\omega_i\tau_i}\left(j_x - n_e e v_x\right)$$

to

$$-j_\theta = j_x\omega_e\tau_e\left(1 - \frac{n_e e v_x}{j_x}\right) \tag{5}$$

where the center of mass velocity v_x in equation (5) does not include the motion of neutrals. For small values of ion flow, equation (5) assumes the familiar form

$$-\frac{j_\theta}{j_x} = \omega_e\tau_e \tag{6}$$

Equation (A2) for j_x changes for negligible ion slip from

$$j_x = n_e e\,\frac{\dfrac{1 + 2\omega_e\tau_e\omega_i\tau_i}{\omega_e\tau_e}\,\dfrac{E_x'}{B} + v_x}{1 + \left(\dfrac{1 + 2\omega_e\tau_e\omega_i\tau_i}{\omega_e\tau_e}\right)^2}$$

to

$$j_x = \left(n_e e v_x + \frac{n_e e}{\omega_e\tau_e}\,\frac{E_x'}{B}\right)\left[\frac{1}{1 + \left(\dfrac{1}{\omega_e\tau_e}\right)^2}\right] \tag{7}$$

Solving equation (7) for v_x and substituting into equation (5) for j_θ, gives

$$-j_\theta = n_e e\,\frac{E_x'}{B} - \frac{j_x}{\omega_e\tau_e} \tag{8}$$

Equation (1) indicates that the inclusion of ion motion will reduce the value of j_θ/j_x below $\omega_e\tau_e$ and equation (8) shows that with increasing $\omega_e\tau_e$

$$-j_\theta \to n_e e\,\frac{E_x'}{B} \tag{9}$$

Noting that for large $\omega_e\tau_e$ values j_x in equation (7)

$$j_x \to n_e e v_x \tag{10}$$

the limiting value for j_θ/j_x is

$$-\frac{j_\theta}{j_x} \rightarrow \frac{E_x'}{B}\frac{1}{v_x} \tag{11}$$

Since for the loss-free case the ions are electrostatically accelerated,

$$v_x = \sqrt{\frac{2eV}{m_i}}$$

Assuming $E_x' l = V$

$$-\frac{j_\theta}{j_x} \rightarrow \sqrt{\frac{E_x'}{l}}\frac{1}{B}\sqrt{\frac{m_i}{2e}} \tag{12}$$

Equation (12) shows how much j_θ/j_x will be reduced below the increasing $\omega_e\tau_e$ as the losses decrease with increasing B, if an increase in the flow of ions is allowed. The transition to smaller losses as B increases beyond the Hall current peak in figure 4 is, however, most unlikely in the present experiment.

Another possibility for a decrease in j_θ/j_x with B after the peak, for a constant j_x, can be explained from equation (8) in terms of a decrease in τ_e or a decrease in n_e with increasing B (assuming that E_x'/B is constant or increases). Since

$$\tau_e = \frac{\lambda}{\bar{c}} = \frac{1}{\sum nQ}\frac{1}{\bar{c}}$$

a decrease in τ_e, barring an increase in n_e (which would also decrease j_θ), would require an increase in the collision cross section. The possibility of such a decrease will depend very much on T_e and the degree of ionization, which help to determine whether elastic collisions of electrons with neutrals, or with ions (Coulomb collisions), or inelastic ionizing collisions predominate. Of course, a check has to be performed if such changes in τ_e and n_e could agree with the experimental variation of E_x' with B for high values of j_x = Constant where the ionization is high enough so that the ion-slip term may perhaps be neglected. The study of the simplified equations excluding ion-slip losses may have certain advantages, however, even for low ionization since the crux of the studies at this stage is the hope to find some simple mechanism, which might explain the experiments. For an explanation of reduction in j_θ as B increases, the exclusion of ion-slip losses complicates matters and the reduction in τ_e, together with a decrease in n_e, does not seem a good possibility,

at least for the present experiments. Of course, more measurements are required, to make sure.

In looking for simple effects the influence of rotation also has to be considered. For the neglect of ion slip the rotation appears only in the term $E_x' = E_x - v_\theta B$. It must be remembered again that E_x is the measured quantity so that $v_\theta B$ could reduce j_θ with increasing B. The effect of rotation alone, however, is not well suited to explain the rise and decrease in j_θ/j_x. Experiments with plasma injection and thermionically emitting cathodes have been prepared to study changes in the j_θ versus B variations for highly ionized plasmas, with small ion slip.

EFFECT OF TURBULENT CONDUCTION MEANING OF LINEAR VARIATION OF E_x' VERSUS B FOR TURBULENT AND CONVENTIONAL CONDUCTION

In the theory for turbulent conduction (ref. 11) adapted to the present case in references 9 and 3, two basic assumptions are made. One is that the ions are assumed at rest and, second, the influence of turbulence on j_θ and the possibility of polarization of the oscillations is not taken into account. The neglect of ion motion limits the theory to high-frequency oscillations with frequency larger than the ion cyclotron frequency. The applicability of this restricted theory to the interpretation of comparatively low frequencies at high magnetic fields (ref. 9) thus must be examined in detail. Recently the theory developed in reference 11 has been extended in reference 12 to include ion motion, and the result was obtained that ion motion greatly reduces the effect of turbulent conduction. This result seems in contrast to the discussion for the growth of many instabilities (and not developed turbulence) for plasmas in magnetic fields in reference 12 and the particularly relevant instability in reference 13 where the presence of ion motion is essential for such growth. While it would, of course, be most desirable if the ions could reduce the effects of turbulent conduction, much more work is necessary to study the instabilities and the turbulent conduction across a magnetic field including a directed motion of ions in the electric field and the effect of neutrals and the related ion slip.

Next, the influence of turbulence on the azimuthal Hall current j_θ, is evaluated. For this purpose, the basis for the development of the theory for turbulent conduction in reference 11 has to be briefly discussed. The theory deals in essence with turbulent conduction and diffusion assuming isotropic turbulence. It can be regarded as a limiting case for small random nonuniformities for the theories of conduction in plasmas with distributed nonuniformities in the presence of Hall effects; these theories were independently developed in references 14 and 3. In these theories which are so strongly dependent on the Hall effect it is logical to include the effect of nonuniformities on the Hall current itself. The necessity for the inclusion of nonuniformities in the Hall current was also experimentally established in reference 6.

To determine in what manner the nonuniformities should affect the Hall current, the effect on turbulence on j_x as discussed in the literature is discussed first. Adaptation of the theory in reference 11 to the present case yields (NOTE: the inclusion of ion oscillations and ion slip would make the problem too complicated.)

$$j_x = \alpha n_e e \frac{E_x'}{B} + n_e e v_x \tag{13}$$

where α under the neglect of ion motion is given by

$$\alpha = \frac{1}{4} \pi \left\langle (n_e - n_{oe})^2 \right\rangle_{avg} \Big/ n_{oe}^2$$

Comparison with equation (7) for the full ionized case indicates that $\omega_e \tau_e$ has been replaced by a constant $1/\alpha$. The quantity α is assumed to be about 1/15 in references 11 and 9. The possibility also must be considered that the reduction of j_θ with B could be influenced by transition to turbulent conduction. Experiments for a highly ionized plasma, using a preionizer, should help to emphasize the turbulent effects by keeping ion slip small.

The turbulent losses could be introduced into j_θ in formal analogy with equations (5) and (8) for the fully ionized case, with the result

$$-j_\theta = j_x \frac{1}{\alpha} \left(1 - \frac{n_e e v_x}{j_x} \right) \tag{14}$$

and

$$-j_\theta = n_e e \frac{E_x'}{B} - \alpha j_x \tag{15}$$

While such a theory would indicate a reduction in j_θ from the nonturbulent case, an increase in α with B would be necessary to explain the decrease in Hall current. Since an increase in α with B would also influence the E_x' versus B relation in equation (13), the important question also arises if the turbulence differs in the axial and azimuthal direction, that is, is polarized in the magnetic field rather than isotropic. The possibility that the decrease in j_θ corresponds to a transition to turbulence with growing oscillations rather than fully developed turbulence also must be considered, through careful experiments.

Finally, a brief evaluation of the influence of turbulent conduction on the variation of E_x' versus B is made. In the absence of ion motion the conventional conduction across B changed from (see eq. (7))

$$j_x = \frac{n_e e}{\omega_e \tau_e} \frac{E_x'}{B} = \frac{n_e m_e}{\tau_e} \frac{1}{B^2} E_x' \tag{16}$$

to (see eq. (13))

$$j_x = \alpha n_e e \frac{E_x'}{B} \tag{17}$$

Assuming constant values for n_e, τ_e, α, and j_x, for conventional conduction

$$E_x' \propto B^2 \tag{18}$$

while for turbulent conduction

$$E_x' \propto B \tag{19}$$

It should be noted in this connection that some curves in figure 6 representing the variation of E_x' versus B could, with a little imagination, be interpreted as showing transition from square to a linear dependence for the higher currents. This transition seems to occur approximately for values of B where the Hall current begins to drop in figure 4. As noted before, however, since the drop in Hall current does not seem to fit into existing turbulent theory, excluding the influence on j_θ, the possibility of polarization and the effect of ion motion would have to be studied to evaluate what could be very important effects in turbulence. The effect of ion motion has also a very simple influence for $n_e e v_x = \text{Constant}$ since as v_x increases n_e is decreased, which in turn can change the term $\alpha n_e e E_x'/B$ and thus the variation of E_x' with B.

Thus the importance of obtaining a better theory and more measurements for turbulent conduction including ion motion across B in the presence of neutrals and for turbulence in the azimuthal direction of the Hall current is very evident. Before such advances are made, the influence of turbulence is difficult to assess, except with many more careful measurements. This, of course, does not mean that means for delaying transition to turbulence may not be found before turbulence is fully understood. Theoretical reasoning (ref. 3) and experiments and theory for other discharge-magnetic-field instabilities (ref. 15) suggest that increased ionization, with resulting reduction in E_x', should give such a delay. Proof has to wait for experimental results.

The question also arises, if the change from square to linear dependence of E_x' on B can be explained by other mechanisms then the transition from conventional to turbulent conduction. A deviation from the parabolic characteristic can also be interpreted in terms of ion slip, since the latter is a loss which reduces the impedance due to high Hall currents alone, which is the basis for the parabolic characteristic. This reduction in impedance occurs in essence for $\omega_i \tau_i \leqq 1$, since for $\omega_i \tau_i > 1$ a related increase in impedance as occurred originally due to $\omega_e \tau_e > 1$ sets in, with resulting tendency again toward $E_x' \propto B^2$. (NOTE: $v_\theta B$, due to rotation can modify the effect.) Since most of the experiments performed so far in the Hall accelerator are in the range of $\omega_i \tau_i \leqq 1$, the

change from square dependency and even a transition to approximately linear dependency could be possible, especially if the possibility of variations in τ_e, t_i, and n_e are also included.

Finally, it should be noted that an interesting attempt has been made in reference 16 to explain a linear variation of E_x' versus B for neglect of ion-slip losses. Then in accordance with equation (16), using a constant j_x

$$\frac{n_e}{\tau_e} \propto B$$

The proportionality is explained through an increase of n_e with B. This increase in ionization with B is explained by the fact that the plasma is partially ionized and that T_e is in such a range that most collisions occur with neutrals and most energy is put into ionization at E_x' increases with B.

It would seem very useful to include the effects of ion slip in this theory to see if at least for partially ionized plasmas at not too high percent ionization a linear variation of E_x' vs. B could be obtained without invoking turbulence. (NOTE: The effectiveness of the preionizer on the accelerator has to be carefully studied in this connection.)

A careful distinction between oscillations introduced at the electrodes and in the discharge will have to be made in the experiments.

APPENDIX A

Ohm's law in the presence of a magnetic field can be written (ref. 6 or ref. 7, where the factor 2 with the term $2\omega_e\tau_e\omega_i\tau_i$ is not considered);

$$\vec{j} = \frac{\sigma_o}{(\omega_e\tau_e)^2 + (1 + 2\omega_e\tau_e\omega_i\tau_i)^2} \left\{ (1 + 2\omega_e\tau_e\omega_i\tau_i)\vec{E'} - \frac{\omega_e\tau_e}{B}(\vec{E'} \times \vec{B}) \right.$$

$$\left. + \left[\left(\frac{\omega_e\tau_e}{B}\right)^2 + \frac{\omega_e\tau_e\omega_i\tau_i}{B^2}(1 + 2\omega_e\tau_e\omega_i\tau_i)(\vec{E'} \cdot \vec{B})\vec{B} \right] \right\} \tag{A1}$$

In the linear Hall accelerator E_r, E_θ, v_r, v_θ, B_x, and B_θ are all taken as zero. Noting that

$$\frac{\sigma_o}{\omega_e\tau_e} = \frac{n_e e}{B}$$

and defining

$$W = \frac{1 + 2\omega_e\tau_e\omega_i\tau_i}{\omega_e\tau_e} = \frac{1}{\omega_e\tau_e} + 2\omega_i\tau_i$$

The expressions for j_x and j_θ are

$$j_x = n_e e \frac{W\frac{E_x'}{B} + v_x}{1 + W^2} \tag{A2}$$

$$-j_\theta = n_e e \frac{\frac{E_x'}{B} - Wv_x}{1 + W^2} \tag{A3}$$

$-j_\theta$ is used since the Lorentz force in the axial direction is $-j_\theta B_r$. Three other expressions for $-j_\theta$ can be found by eliminating E_x', v_x, and n_e from the above equations

$$-j_\theta = \frac{1}{W}(j_x - n_e e v_x) \tag{A4}$$

$$-j_\theta = n_e e \frac{E_x'}{B} - Wj_x \tag{A5}$$

$$-j_0 = \frac{\frac{E_x'}{B} - Wv_x}{W\frac{E_x'}{B} + v_x} \tag{A6}$$

If for j_x constant, τ_e and τ_i are also assumed constant, W will be a function of B only

$$W = \frac{1}{\frac{e\tau_e}{m_e}B} + \frac{2e\tau_i}{m_i}B \tag{A7}$$

and

$$\frac{dW}{dB} = -\frac{1}{\frac{e}{m_e}\tau_e B^2} + \frac{2e}{m_i}\tau_i \tag{A8}$$

$$\frac{d^2W}{dB^2} = \frac{2}{\frac{e}{m_e}\tau_e B^3} \tag{A9}$$

Thus W will have a minimum value at

$$2\frac{e\tau_e}{m_e}B\,\frac{e\tau_i}{m_i}B = 1$$

or

$$2\omega_e\tau_e\omega_i\tau_i = 1 \tag{A10}$$

and at this minimum value

$$W_{min} = \frac{2}{\omega_e\tau_e} \tag{A11}$$

and

$$2\omega_i\tau_i = \frac{1}{\omega_e\tau_e}\bigg|_{W=min} \tag{A12}$$

APPENDIX B

METHODS OF PREIONIZATION

Reasons for Preionization

As pointed out in the discussion of turbulent conduction in the body of the paper, the effect of preionization is not only to increase the number of ions being accelerated. Its function is also to delay the onset of instabilities and transition to turbulent conduction by reduction of the voltage which provides energy for the growth of instabilities and turbulence. Two methods of preionization will be discussed. One makes use of a coaxial preionizer with magnetic field which injects a plasma stream into the accelerator. Such a preionizer has been designed and operated. The second method of preionization is actually a method for supplementary ionization in the accelerator region itself. Such an approach has been tried for delaying the onset of instabilities of an arc column in an axial magnetic field (ref. 15) and will be applied to the present Hall-ion accelerator.

Design and Operation of Arc Preionizer

J. Burlock and T. Collier

(a) Method and Design

Most preionizers for the low-density plasma accelerators consist of some form of PIG discharge with externally heated thermionically emitting cathodes. In order to obtain a highly ionized plasma, the use of high currents in the preionizer becomes desirable; for that purpose it has to operate in the arc mode. For injection into the Hall-ion accelerator with a center core it is furthermore desirable to produce a plasma stream which is concentrated, more or less, in a cylindrical annulus.

These various requirements suggested the use of a tungsten disc cathode self-heated by the arc discharge inside a ring anode. The design is shown in figure 10. The arc discharge establishes itself mainly in the space between the edges of the disc and the anode and is blown into the accelerator. The edges of the disc can act as an electric field concentrator and facilitate the starting and act to maintain the discharge in this position. The magnetic field can be purely axial or somewhat slanted giving the effect of a Hall current plasma accelerator. The disc cathode was supported by a center sting with much smaller diameter, which resulted in uniform heating of the cathode disc, since only a small (1/8 inch) spot was cooled by presence of the rod. The major mechanism for removal of heat from the disc was radiation.

Operation

Typical operation of the disc cathode is shown in the accompanying illustrations. A high-voltage low-current glow discharge produces the initial heating. A rapid shift to high-current operation follows as the cathode reaches emitting temperature. The cathode disc appears uniformly heated except for the central region, where the supporting rod is welded and which shows as a dark spot in the photograph. Operation appeared quite smooth except for occasional appearance of anode spots.

Operation in this instance was in argon at 30 microns pressure, and 15 to 18 amperes at several hundred volts in a magnetic field of 5,000 gauss.

(b) Methods for Supplementary Ionization in Accelerator

J. Burlock

The basic requirement for any technique of ionization enhancement is that the Hall current accelerator mechanism should not be disturbed. Several possible techniques for obtaining the desired ionization will be discussed briefly.

Electrostatic coupling of high-frequency energy directed radially along the flux lines could be used. For frequencies much below plasma frequency, it would be necessary to minimize the impedance of any dielectric intervening between the electrodes and plasma because of the relatively low impedance of a highly overdense plasma. However, if leads through the structure are permissible, the electrode could be placed inside, and the dielectric problem would not occur. Electrode cooling in this case would also protect the glass wall.

Inductive coupling of high-frequency energy by means of a solenoid has been used to increase ionization and reduce the axial electric field. The presence of the radial magnetic field of the Hall accelerator transverse to the induced azimuthal electric field hinders the coupling of energy, and relatively high powers are required to produce appreciable changes in conductivity and axial electric field. Operation at electron cyclotron resonance frequency would provide an important coupling enhancement. For this operation the magnetic fields of interest for the acceleration process, with intensities hundreds of gauss and higher, would call for power at frequencies in the order of hundreds to several thousand megacycles. A reasonable upper limit for the resonance technique could be at between one and two thousand gauss, where high power at the corresponding cyclotron resonant frequencies (in the kilomegacycle range) is still reasonably available. Since the electron motion is bidirectional, it should probably not interfere with the undirectional fields and current flows of the accelerating process. It could perhaps provide additional stabilization (ref. 3).

One other possible means of enhancing ionization would be the use of electron ionizing beams, which have proved successful in generating plasmas of reasonably high densities.

APPENDIX C

DESIGN AND OPERATION OF AN EXTERNALLY HEATED RING CATHODE

Olin Jarrett

Most designs for externally heated cathodes for thermionic emission use either a tungsten filament heated by Joule losses due to resistance or a tungsten disc heated by electron bombardment. Since in the Hall accelerator the use of axially symmetric cathode shapes, especially ring cathodes, is highly desirable, another method of cathode heating was tried which ideally seems to suit this purpose. This method of heating also avoids the necessity of vacuum seals for hot external leads.

A RF heated ring cathode has been constructed and tested. The heated cathode (fig. 11) consists of a tungsten ring placed inside of a boron nitride holder which fits into a vycore or quartz tube, inside of which the low pressure is maintained. A connection to the direct-current power supply for operation of the Hall-ion accelerator is provided.

Tests of this device showed that the cathode is uniformly heated to thermionic emission temperature. Since a 20-kw, 450-kc power supply has been available to us, the heating is done with power to spare. The cathode has been installed in an accelerator and the effect on the discharge characteristics will be tested in the near future. Various methods of avoiding possible disturbances of Hall current measurement during such heating have been considered, such as choking the Hall current diagnostic coil, or providing a cathode thick enough to provide sufficient heat capacity for the duration of the Hall current measurement.

The use of a RF heated cathode should also prove very useful in preionizers or axially symmetric plasma accelerators in general.

Tests are also in progress with thick resistance heated ring filaments, such as are used in induction furnaces.

REFERENCES

1. Hess, R. V.: Experiments and Theory for Continuous Steady Acceleration of Low Density Plasmas. Vol. I of Proc. XI Internatl. Astronautical Congress, August 1960, C. W. P. Reuterswärd, ed., Springer Verloy (Vienna), 1961, pp. 404-411.

2. Bratenahl, A., Jones, G. S., and Kantrowitz, A. R.: Plasma Acceleration in the Electromagnetic Region II. Bulletin American Phys. Soc., Ser. II, Vol. 6, No. 4, p. 379, June 1961.

3. Hess, R. V.: Fundamentals of Plasma Interaction With Electric and Magnetic Fields. NASA-University Conference on the Science and Technology of Space Exploration. Vol. 2, paper 59. Chicago, Nov. 1962.

4. Rigby, R. N.: Some Physical Properties of an Axial Electric Arc in a Radial Magnetic Field. M. A. Thesis, The College of William and Mary, Va., Aug. 1962.

5. Hess, R. V., Rigby, R. N., and Weinstein, R. H.: Observation of Hall Currents for a D-C Axial-Arc Discharge in a Radial Magnetic Field. Bulletin American Phys. Soc., Ser. II, Vol. 8, No. 2, p. 168, Feb. 1963.

6. Hess, R. B., Burlock, J., Sevier, J. R., and Brockman, P.: Theory and Experiments for the Role of Space Charge in Plasma Acceleration. Symposium on Electromagnetics and Fluid Dynamics of Gaseous Plasma. April 1961. Vol. XI of Microwave Res. Inst. Symposia Ser., Polytechnic Press of Polytechnic Inst. of Brooklyn, pp. 269-305, 1962.

7. Cann, G. L., Ziermer, R. W., and Marlotte, G. L.: The Hall Current Plasma Accelerator. Electro-Optics, Inc. Presented at the ARS Electric Propulsion Conference, Colorado Springs, Colorado, Mar. 1963.

8. Chen, F. F.: A Time Resolved Probe Method. Plasma Physics Lab., Princeton Univ., MATT 62, Feb. 1961.

9. Jones, G. S., Dotson, J., and Wilson, T.: Electrostatic Acceleration of Neutral Plasmas. Momentum Transfer Through Magnetic Fields. Avco-Everett Res. Lab. AMP 88, Sept. 1962.

10. Salz, F., Meyerand, R. G., Jr., and Lary, E. C.: Ion Acceleration in a Gyro-Dominated Neutral Plasma Experiment. Bulletin American Phys. Soc. Ser. II, Vol. 7, No. 7, p. 441, Aug. 1962.

11. Yoshikawa, S., and Rose, D. J.: Anomalous Diffusion of a Plasma Across a Magnetic Field. The Physics of Fluids, Vol. 5, No. 10, pp. 1272-1277, Oct. 1962.

12. Kadomtsev, B. B.: Turbulent Plasma in a Strong Magnetic Field. Jour. of Nuclear Energy, Part C (Plasma Physics), Vol. 5, pp. 31-36, 1963.

13. Simon, A.: Instability of a Partially Ionized Plasma in Crossed Electric and Magnetic Fields. The Physics of Fluids, Vol. 6, No. 3, pp. 382-388, Mar. 1963.

14. Rosa, R. J.: Hall and Ion-Slip Effects in a Nonuniform Gas. The Physics of Fluids, Vol. 5, no. 9, pp. 1081-1090, Sept. 1962.

15. Gierke, G., and Wöhler, K. H.: On the Diffusion in the Positive Column in a Longitudinal Magnetic Field. Nuclear Fusion Journal of Plasma Physics and Thermonuclear Fusion, 1962 Supplement Part 1 (Salzburg, Sept. 1961), pp. 47-53, 1962.

16. Chubb, D. L.: Hall Current Ion Accelerator. Fourth Symposium on the Engineering Aspects of Magnetohydrodynamics, April 1963 (10-minute paper, only oral presentation).

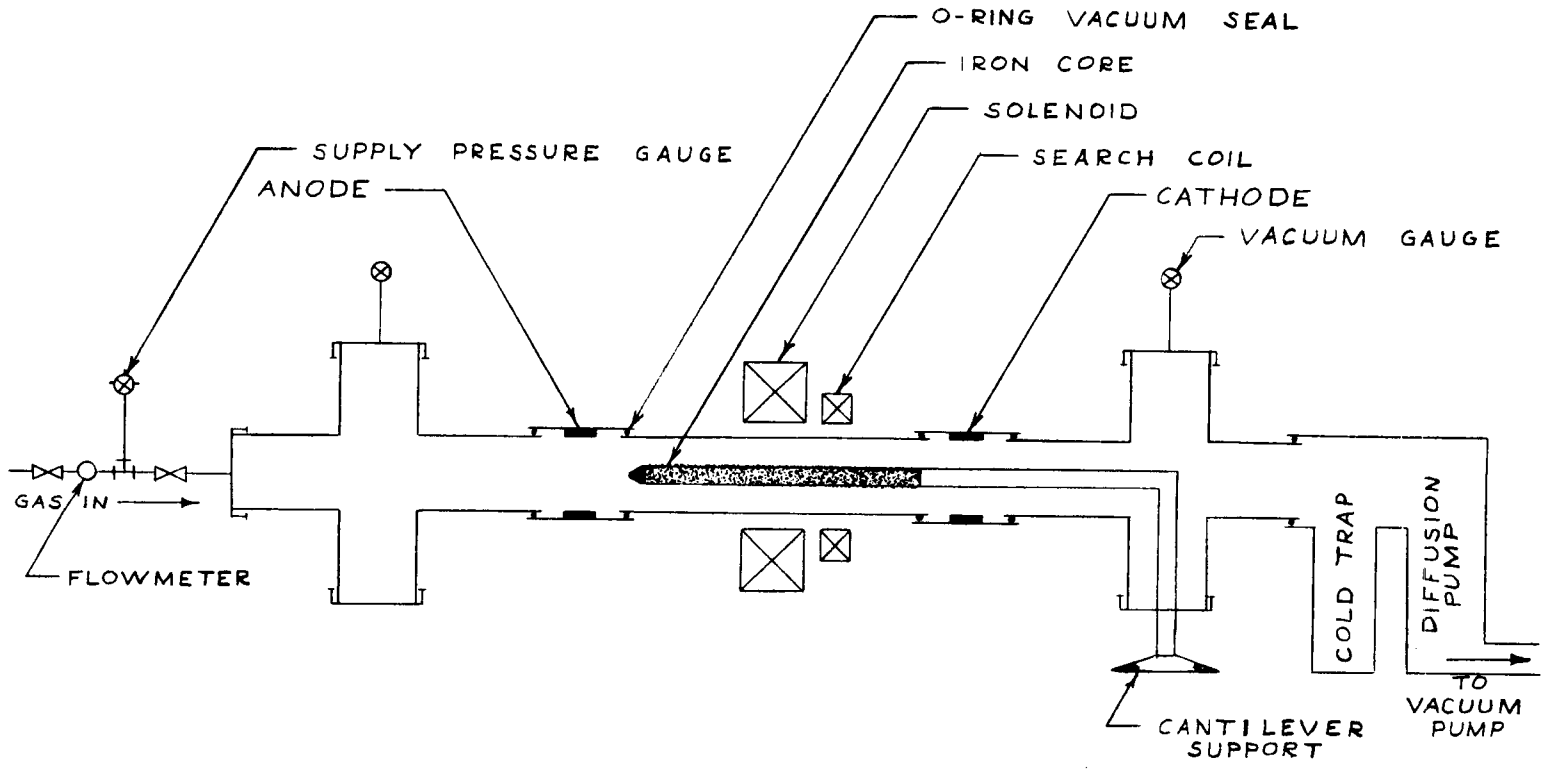

NASA

Figure 1.- Schematic of apparatus.

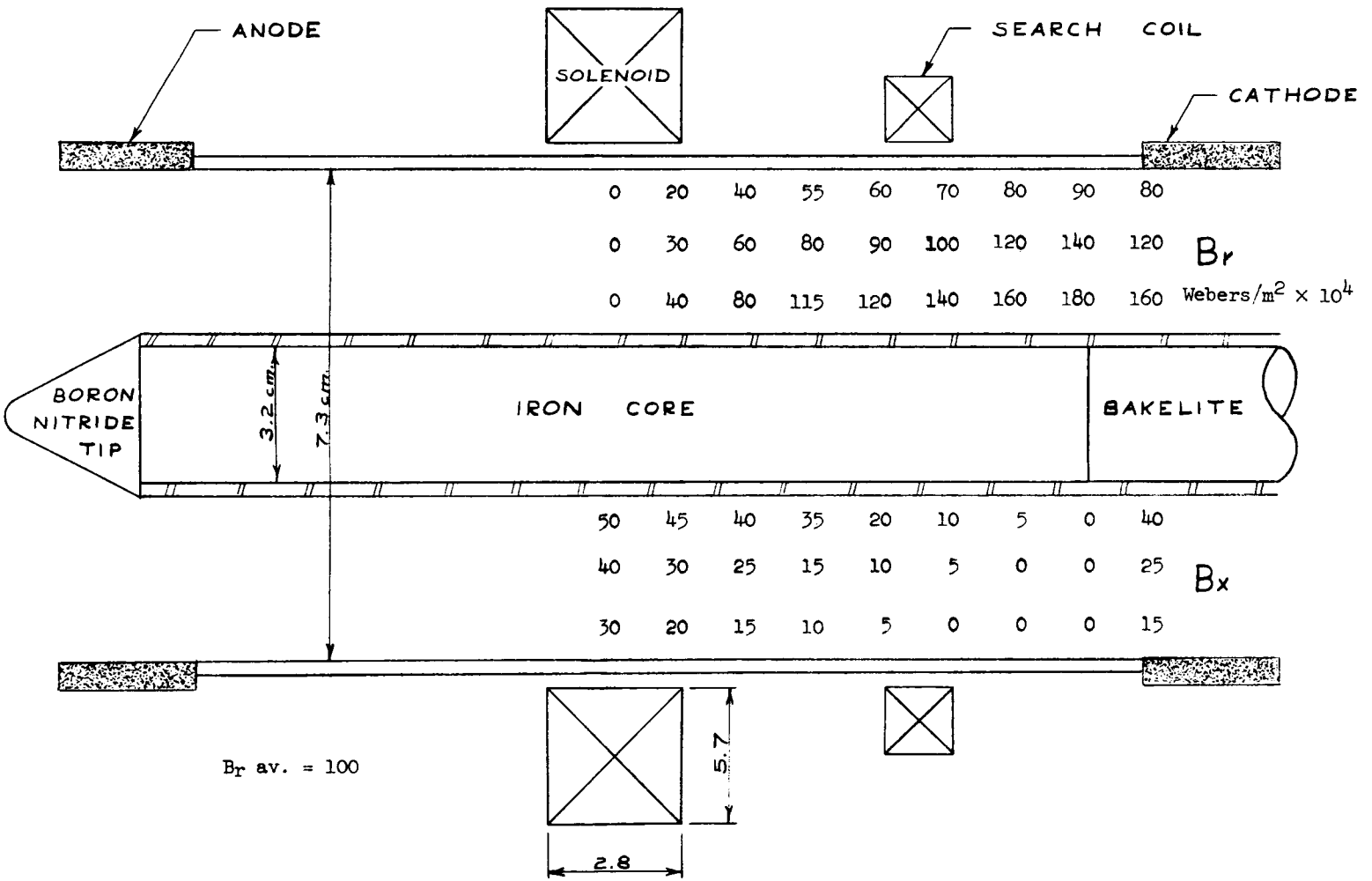

Figure 2.- Schematic of magnetic-field configuration.

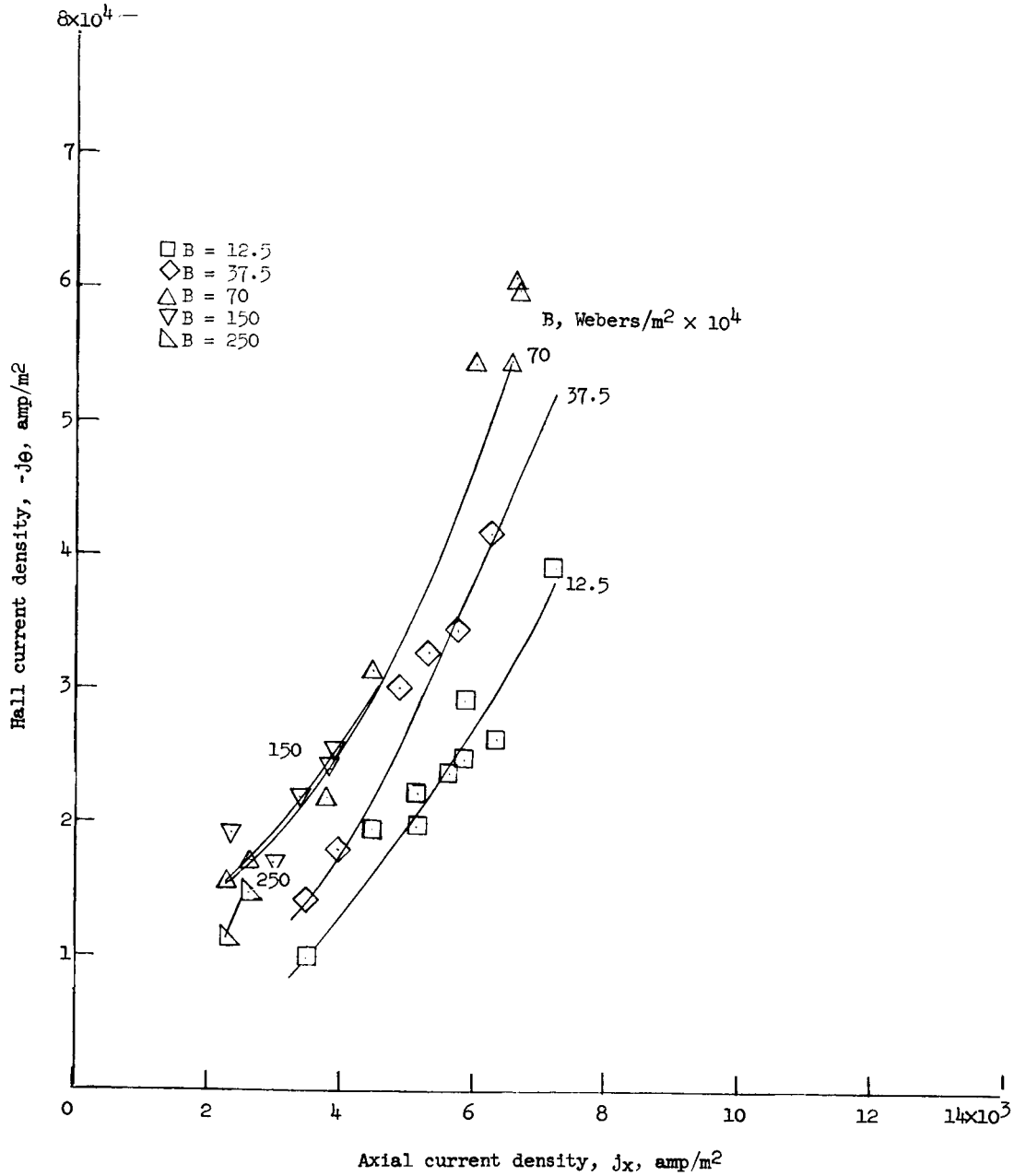

(a) p = 15 μ Hg. NASA

Figure 3.- Hall current density versus axial current density for various magnetic flux densities.

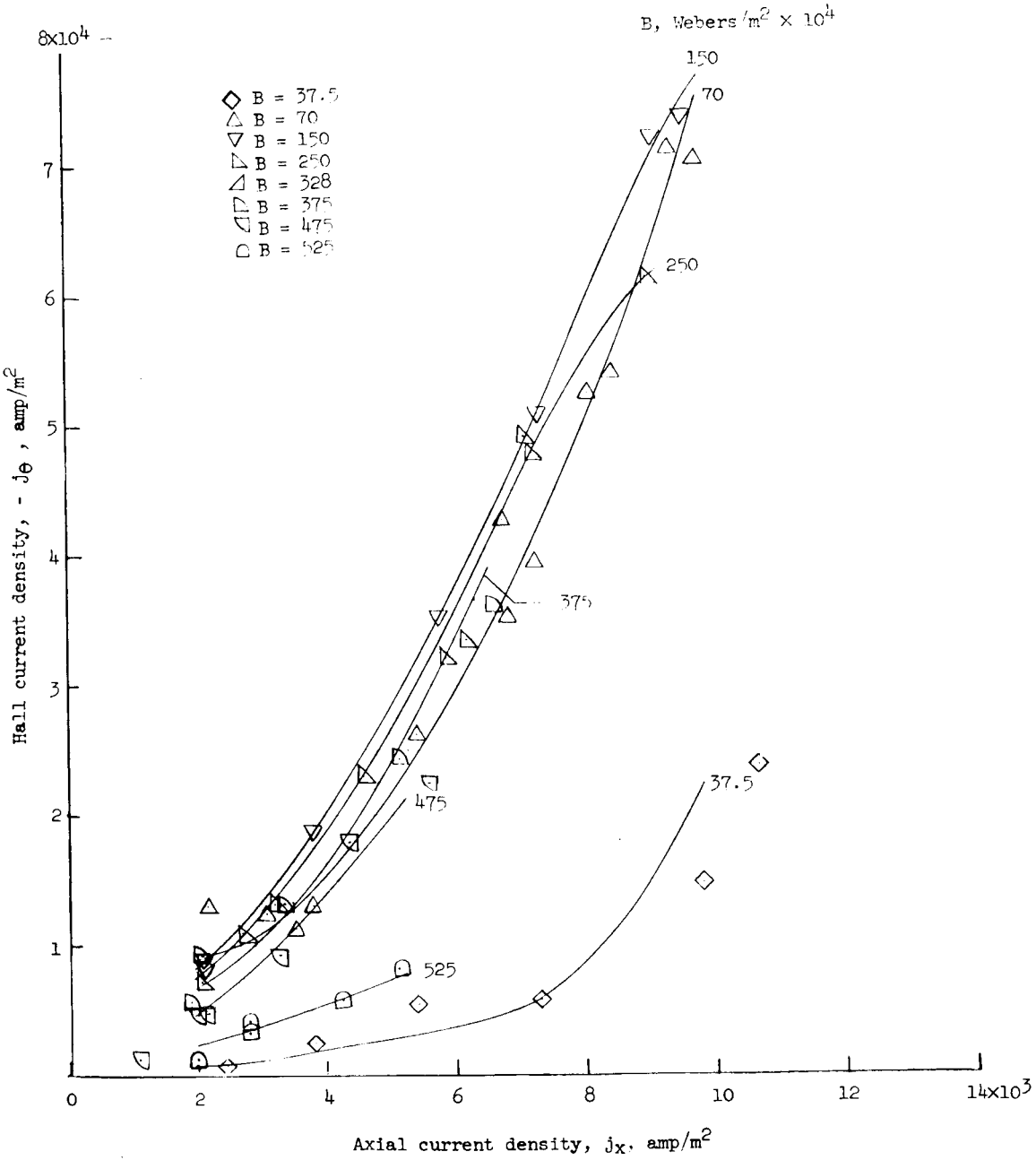

(b) p = 30 μ Hg.

NASA

Figure 3.- Continued.

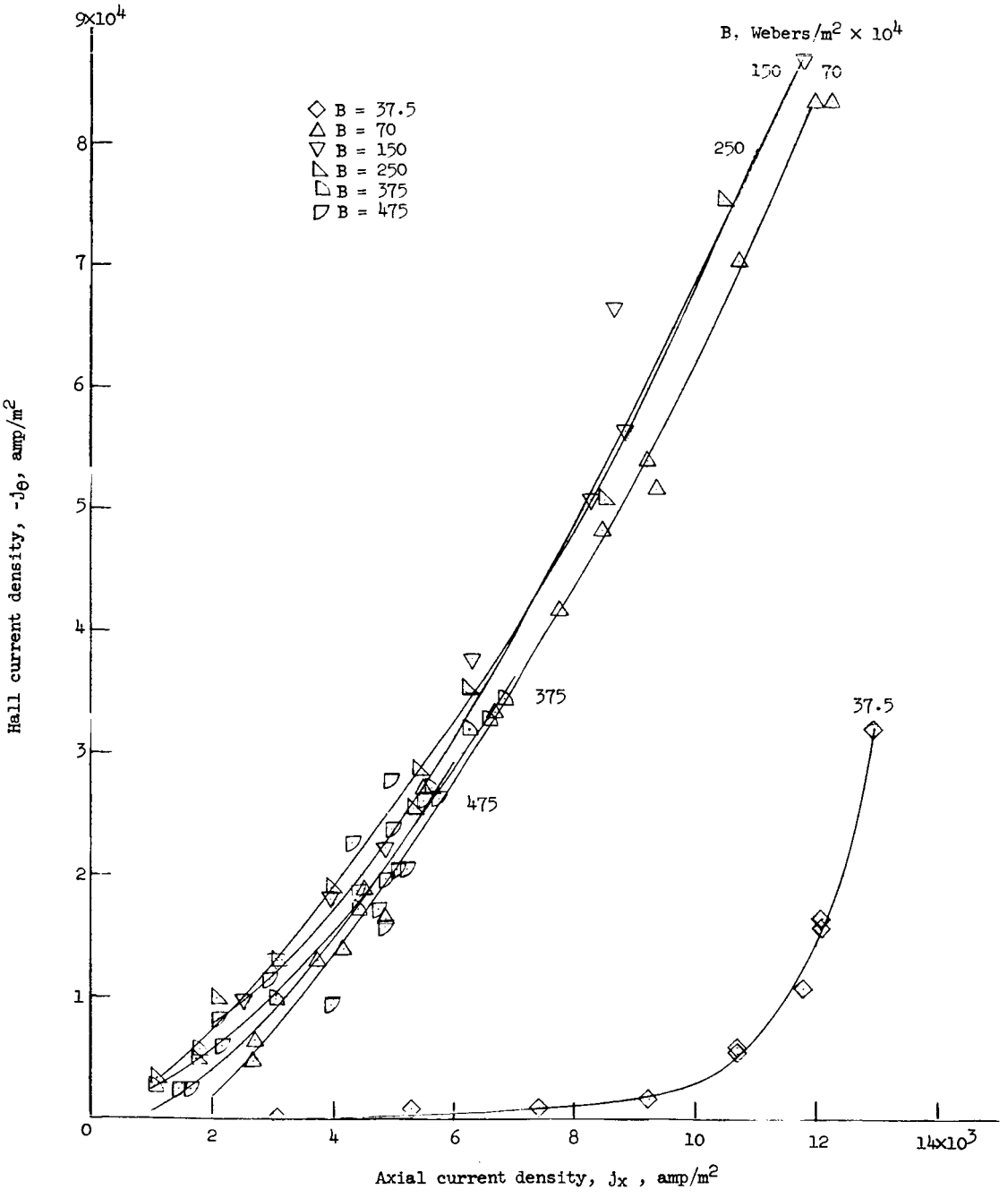

(c) p = 40 μ Hg. NASA

Figure 3.- Concluded.

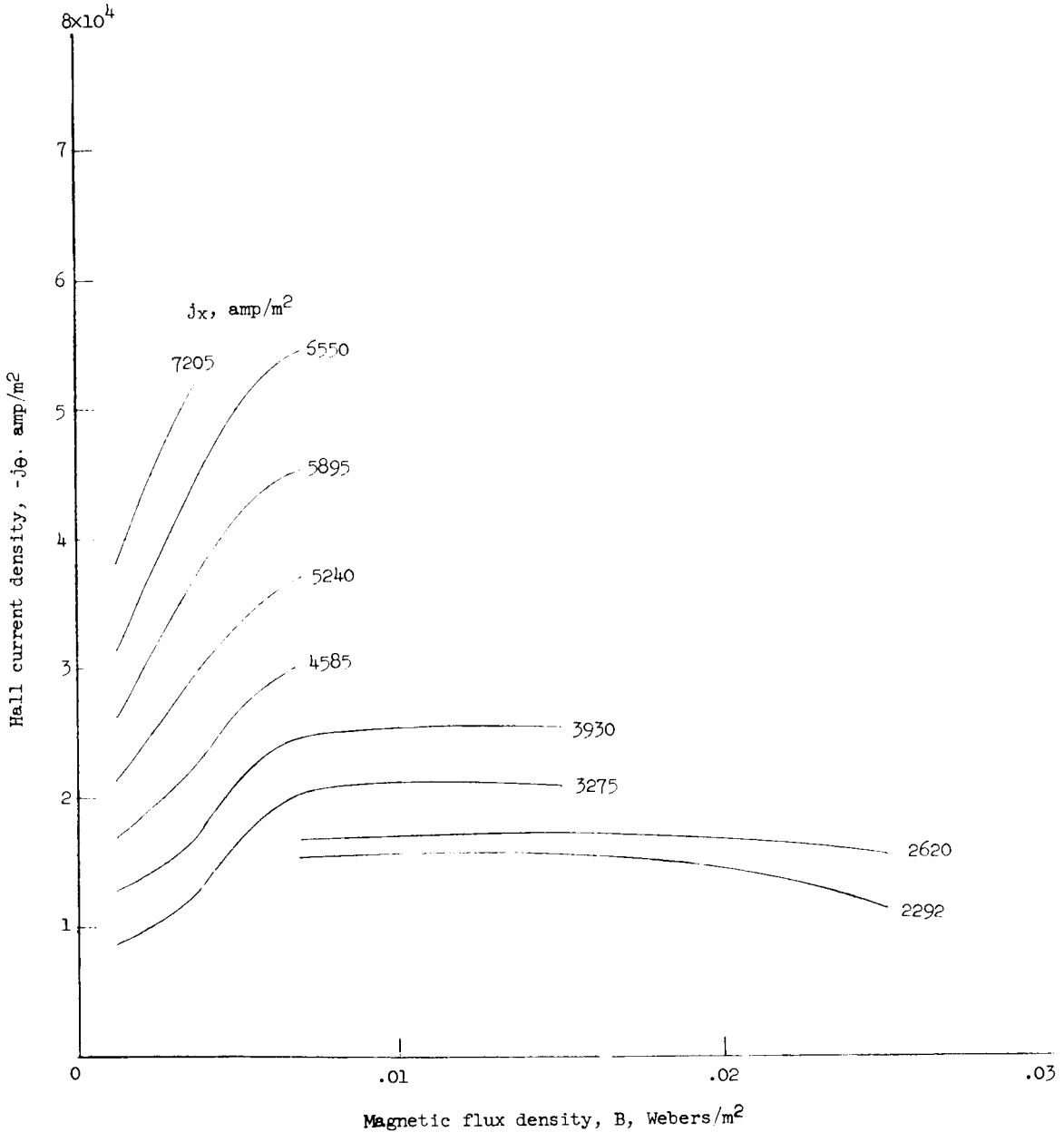

(a) p = 15 μ Hg. NASA

Figure 4.- Hall current density versus magnetic flux densities for various axial current densities.

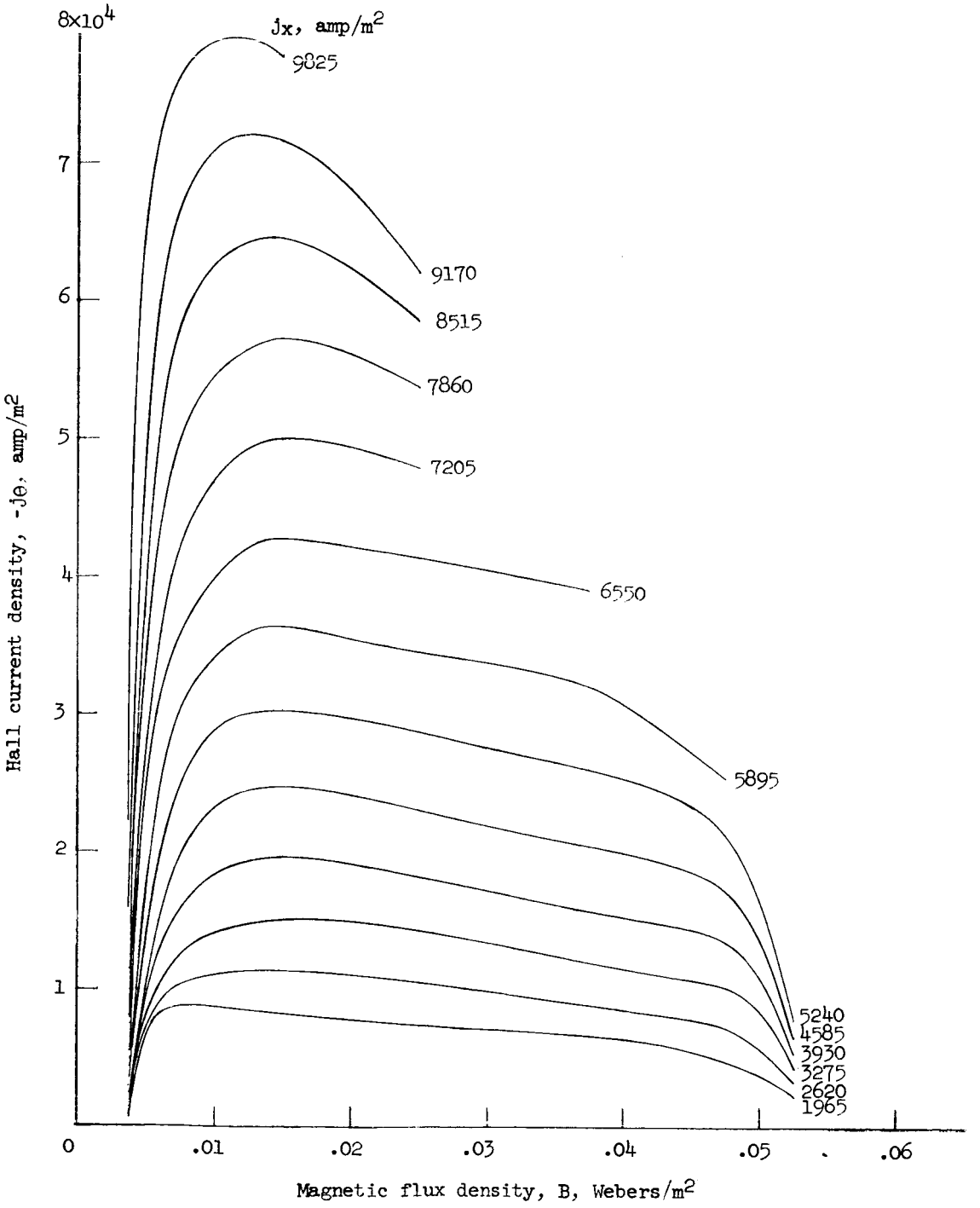

(b) p = 30 μ Hg. NASA

Figure 4.- Continued.

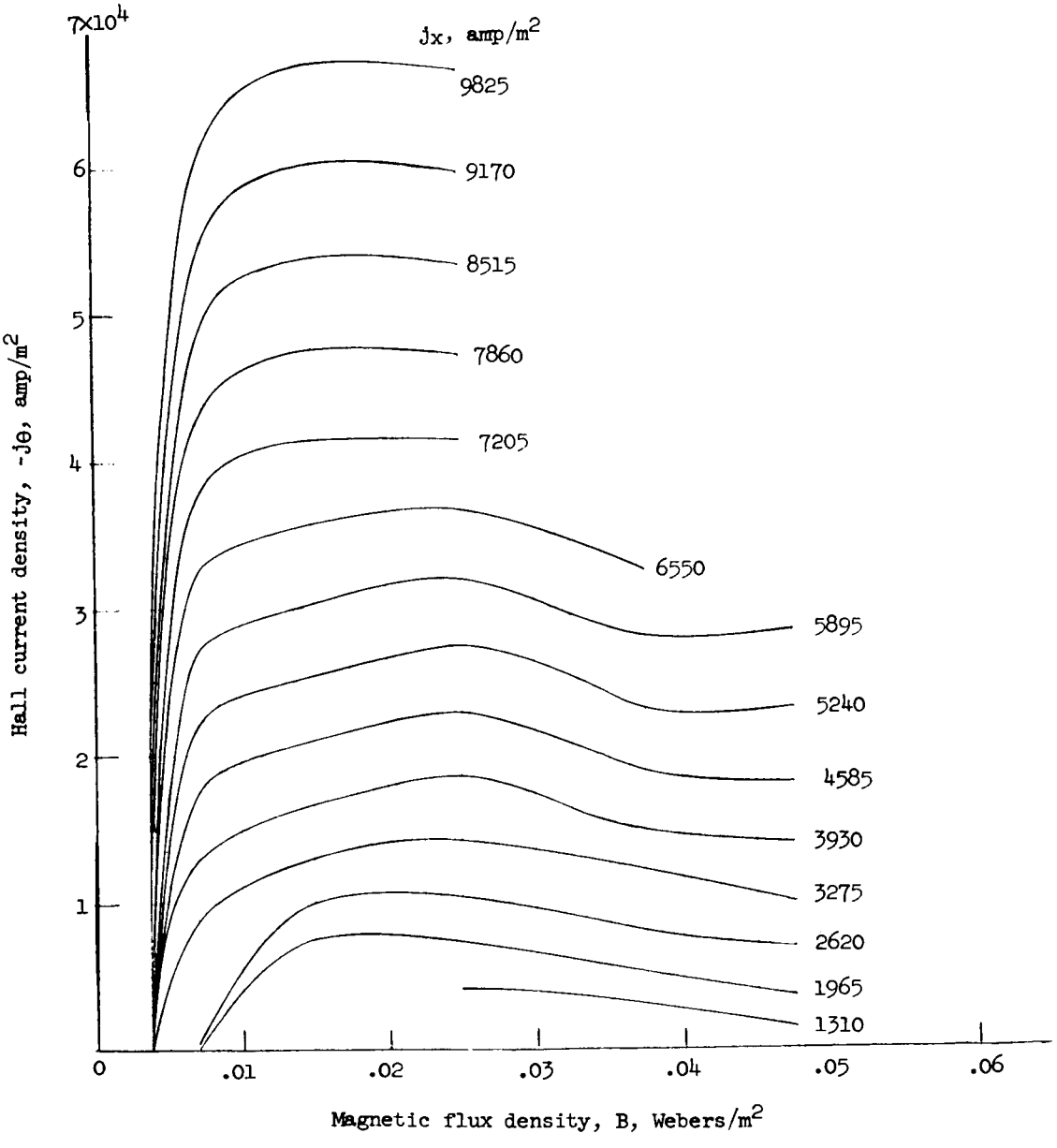

(c) p = 40 μ Hg.

NASA

Figure 4.- Concluded.

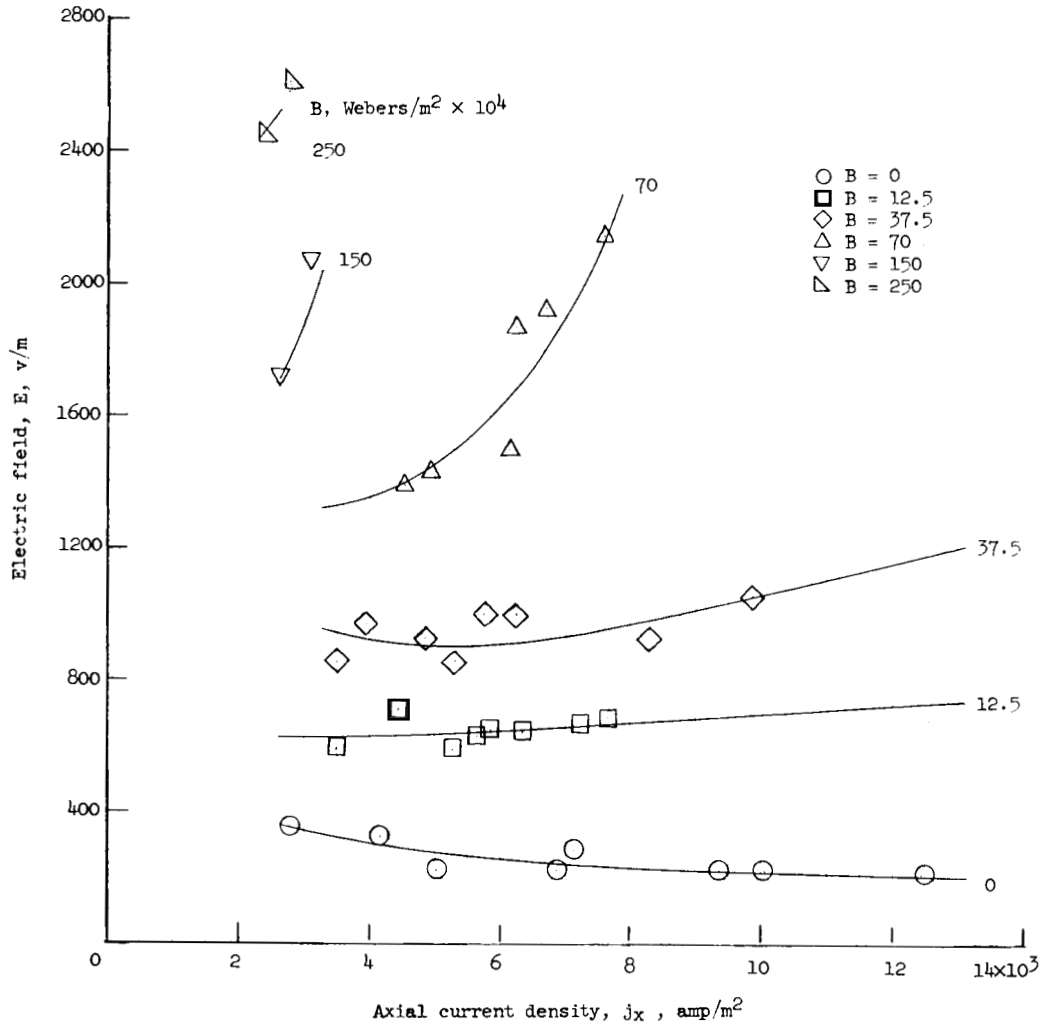

(a) p = 15 μ Hg. NASA

Figure 5.- Electric field versus axial current density for various magnetic flux densities.

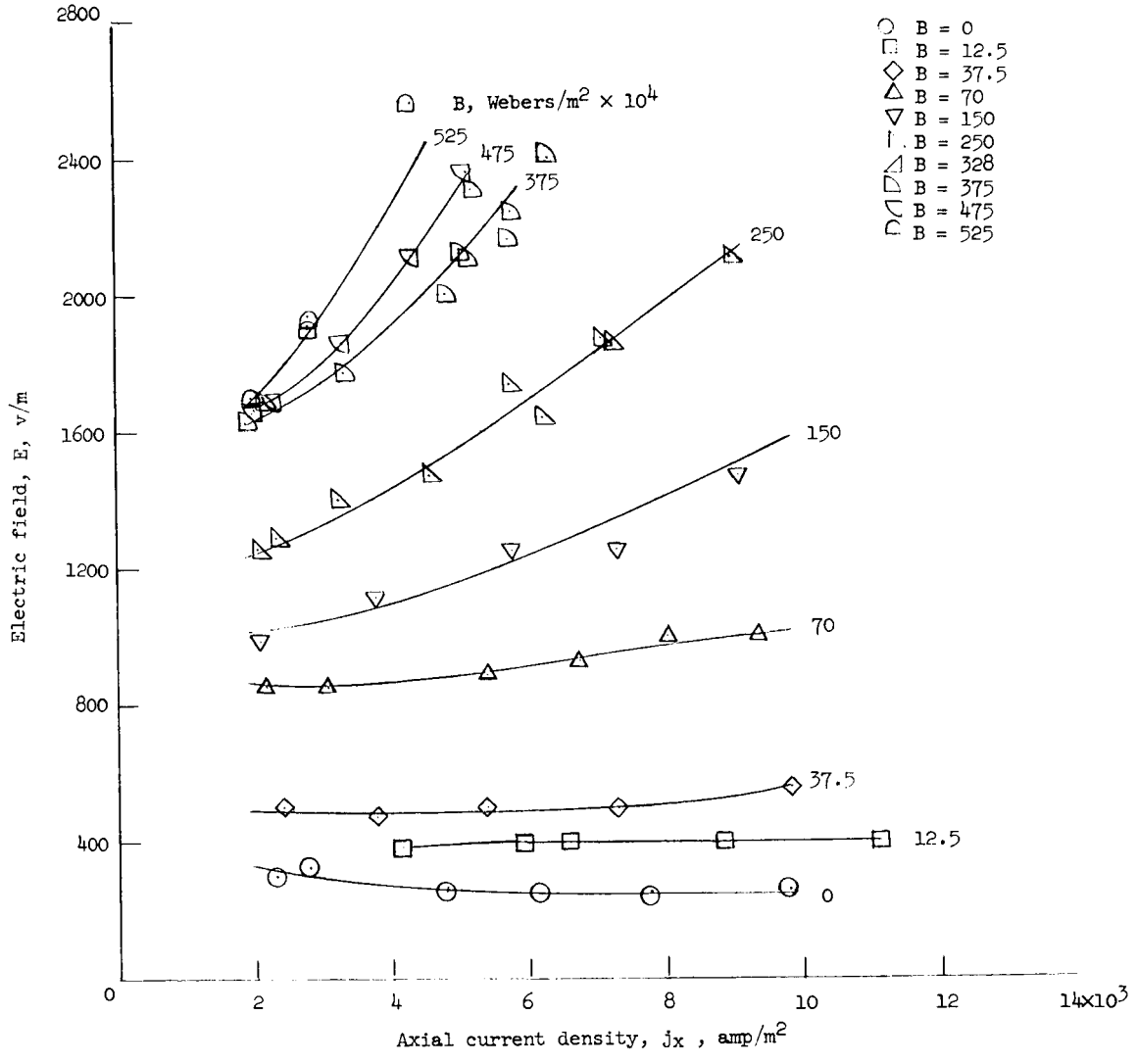

(b) p = 30 μ Hg. NASA

Figure 5.- Continued.

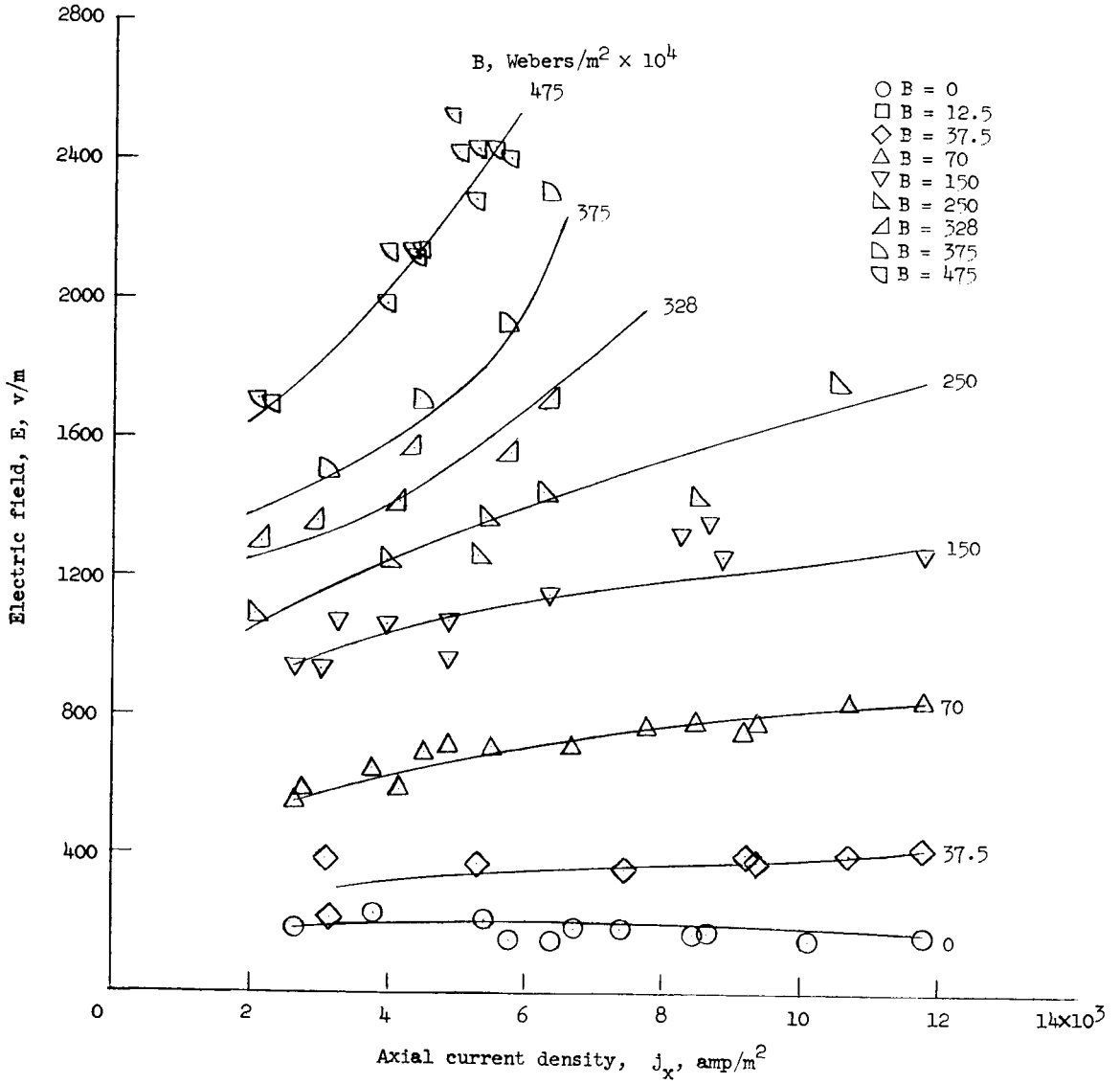

(c) p = 40 μ Hg. NASA

Figure 5.- Concluded.

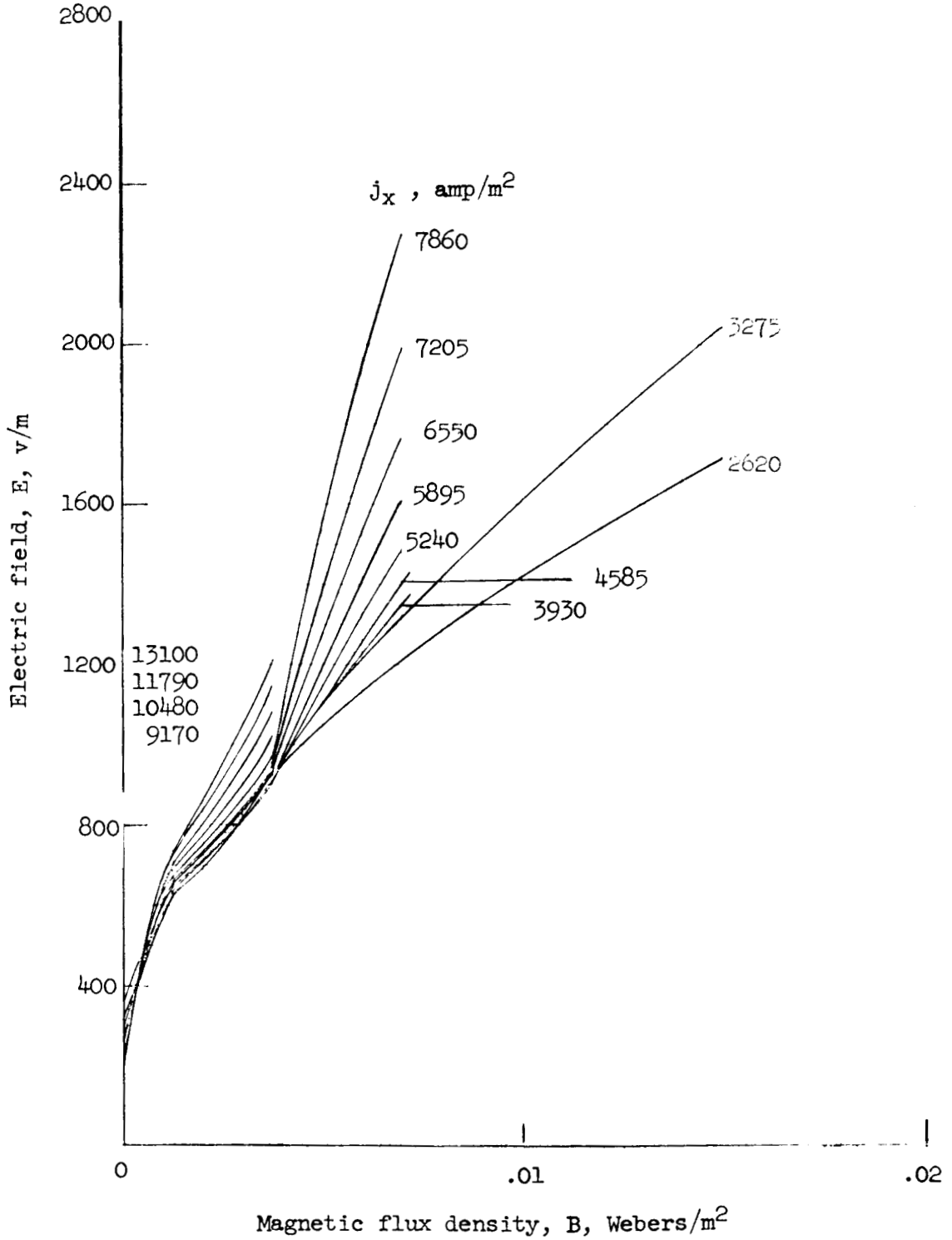

(a) p = 15 μ Hg. NASA

Figure 6.- Electric field versus magnetic field strength for various axial current densities.

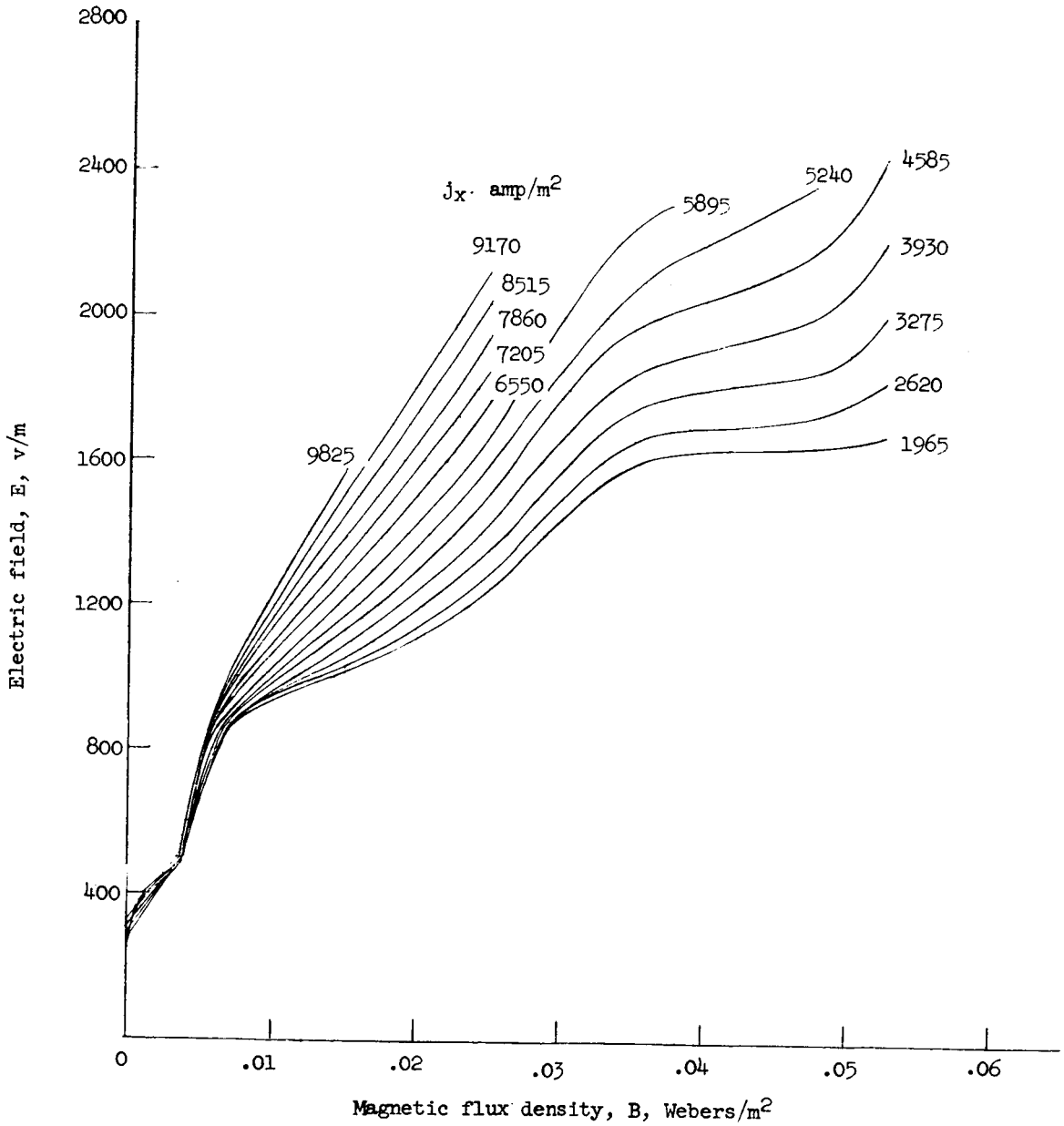

(b) p = 30 μ Hg.

NASA

Figure 6.- Continued.

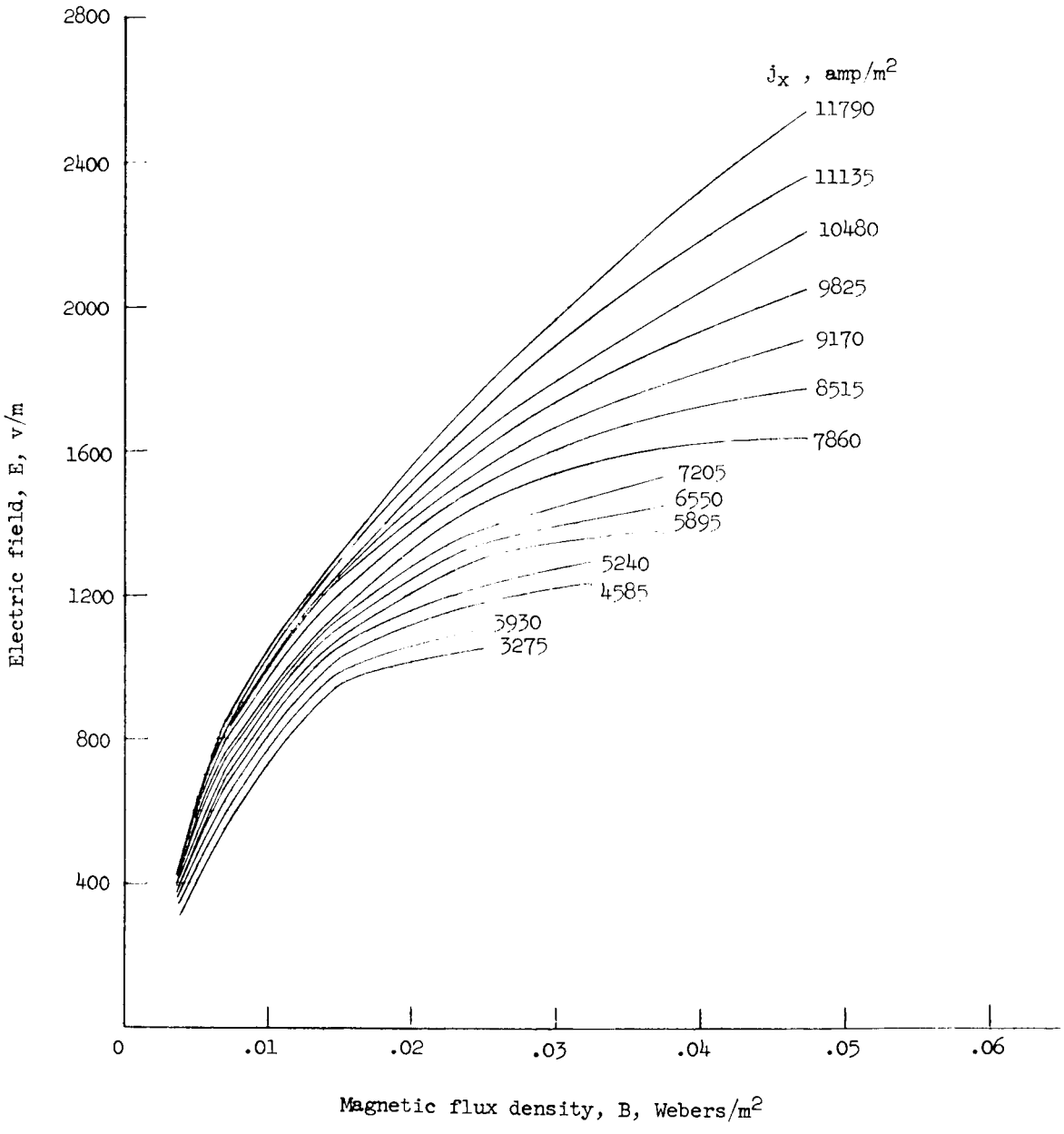

(c) p = 40 μ Hg. NASA

Figure 6.- Concluded.

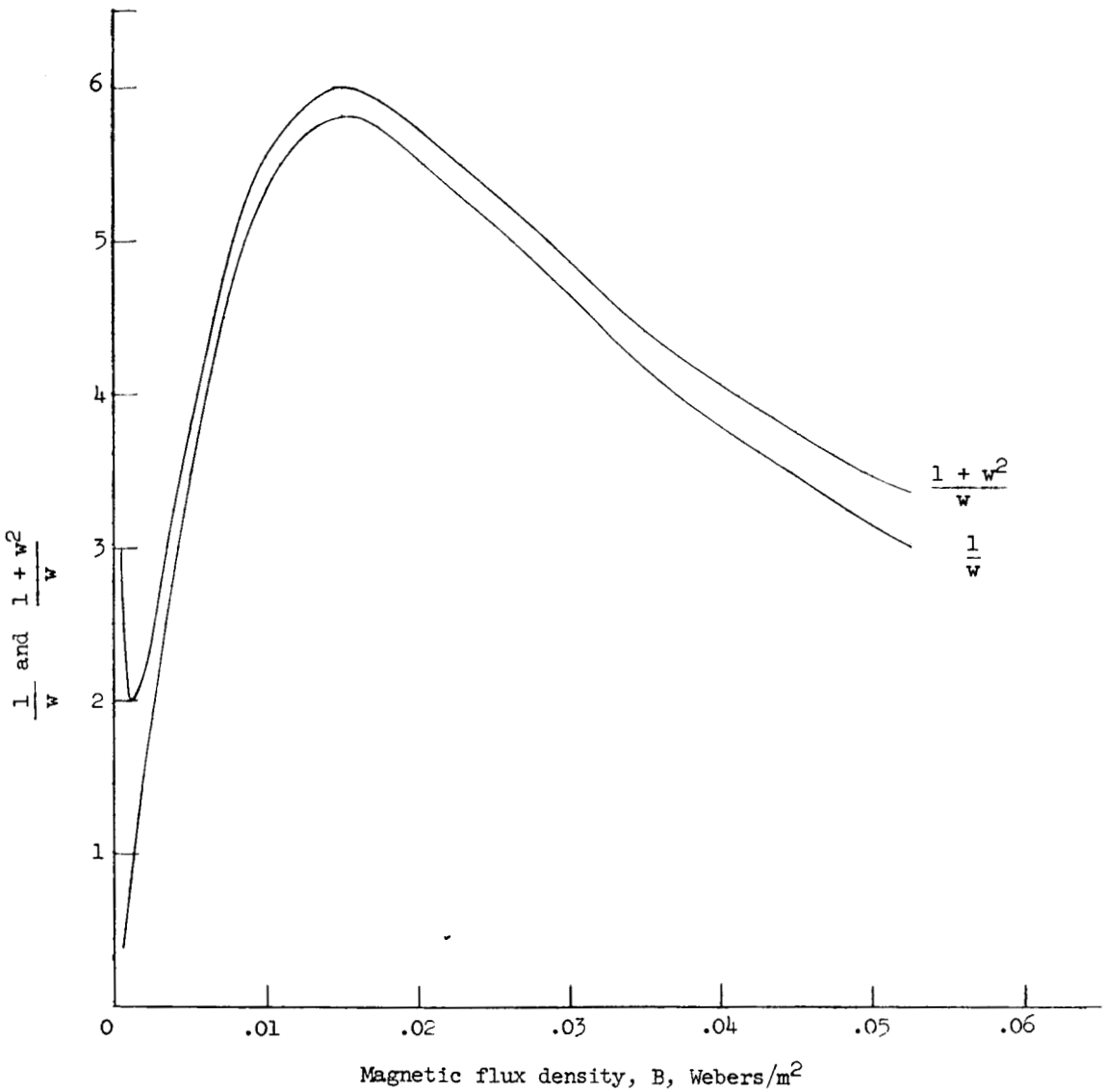

NASA

Figure 7.- Variation of $\frac{1}{w}$ and $\frac{1 + w^2}{w}$ with magnetic flux density.
(p = 30 μ Hg.)

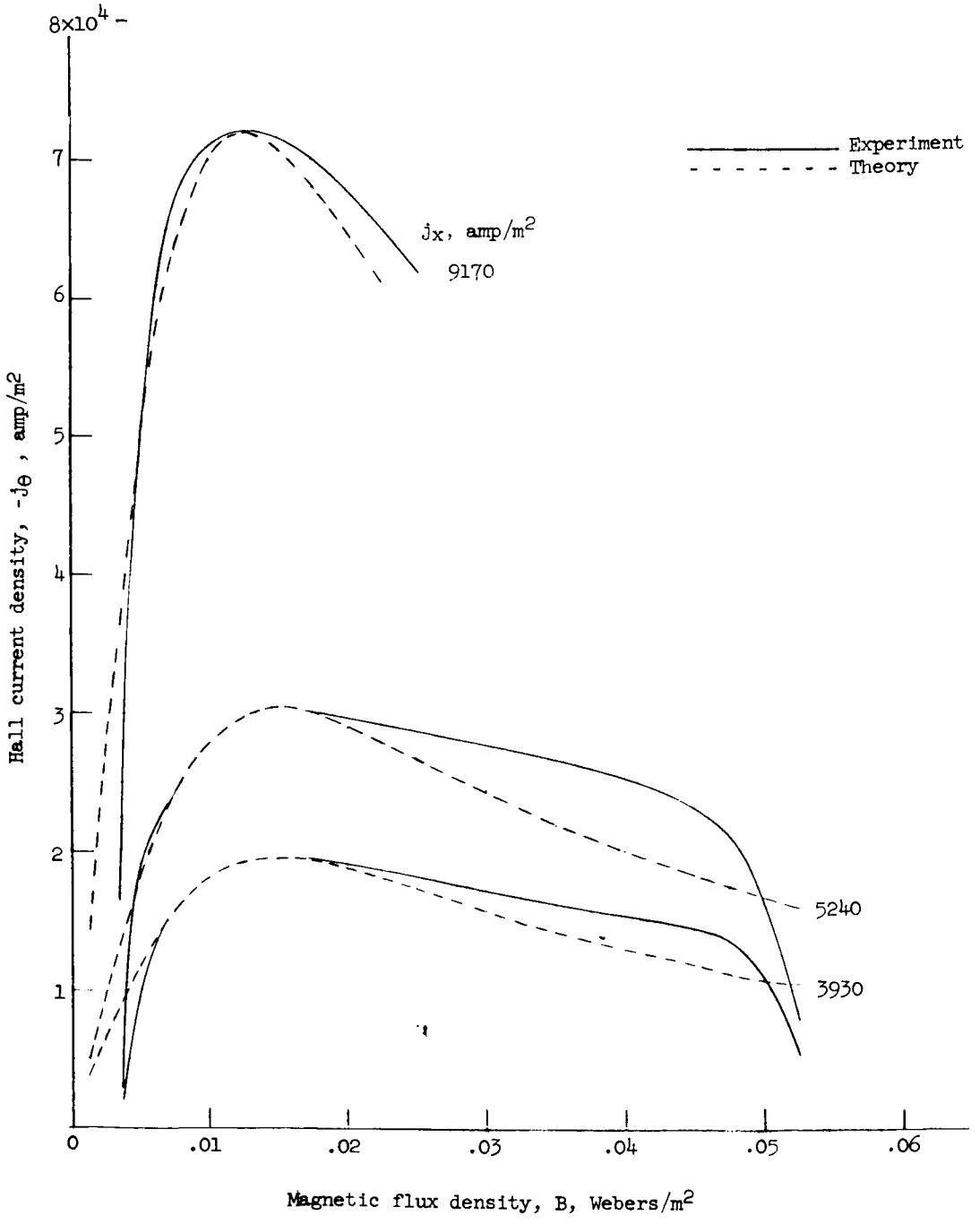

NASA

Figure 8.- Comparison of theory and experiment (Hall current density versus magnetic flux density). p = 30 μ Hg.

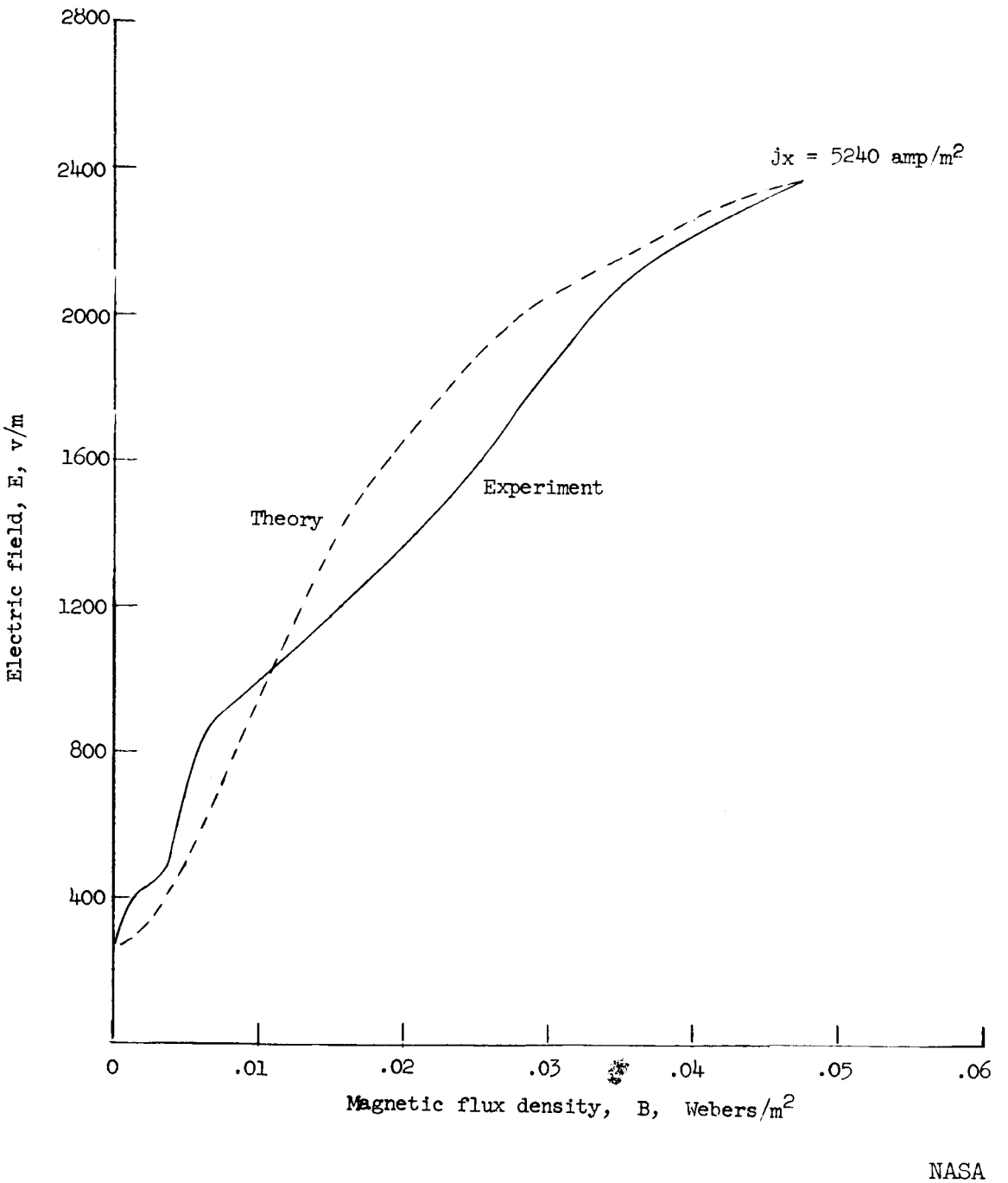

Figure 9.- Comparison of theory and experiment (electric field versus magnetic flux density).

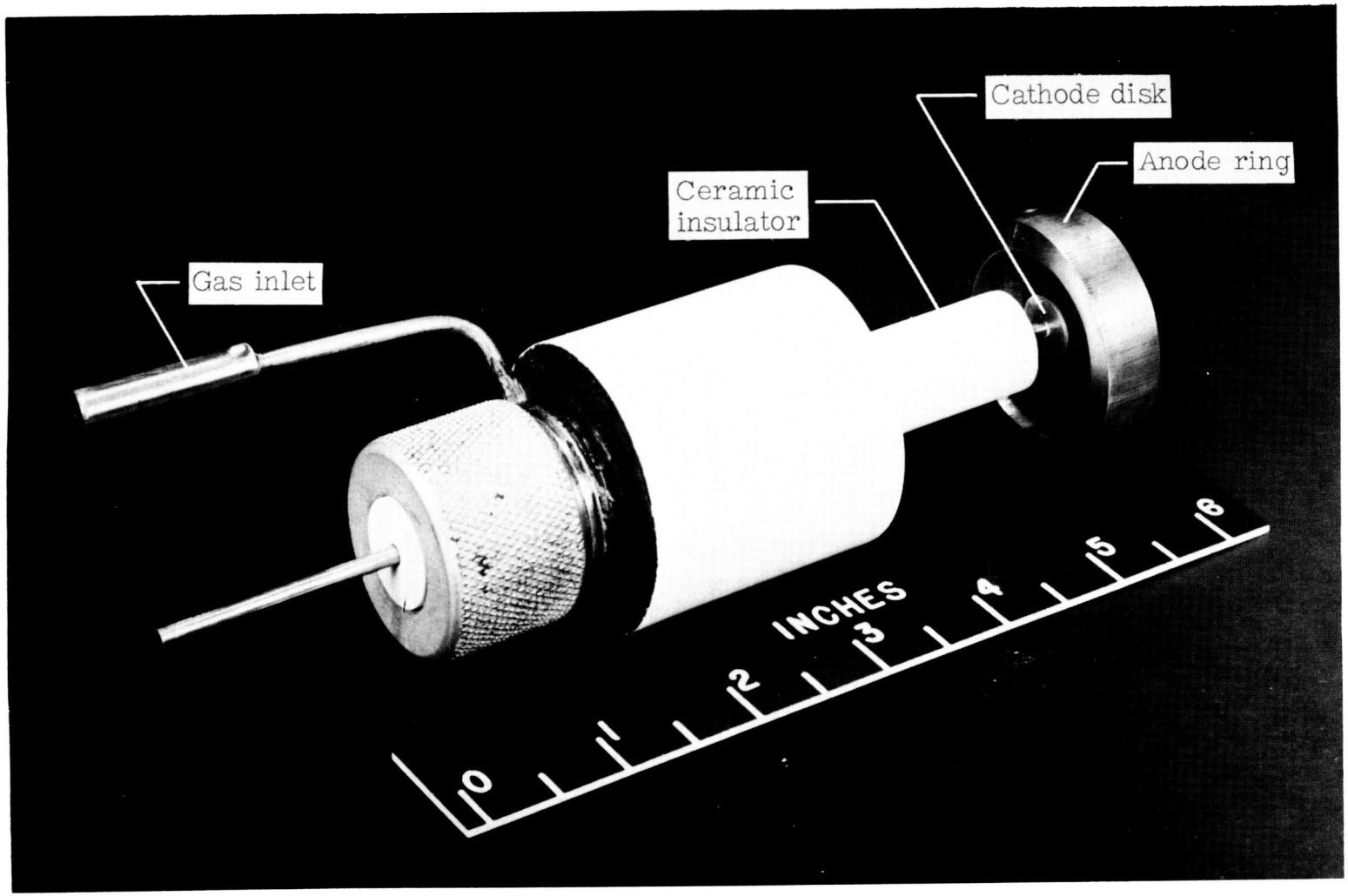

NASA
L-63-3845

Figure 10.- Arc preionizer.

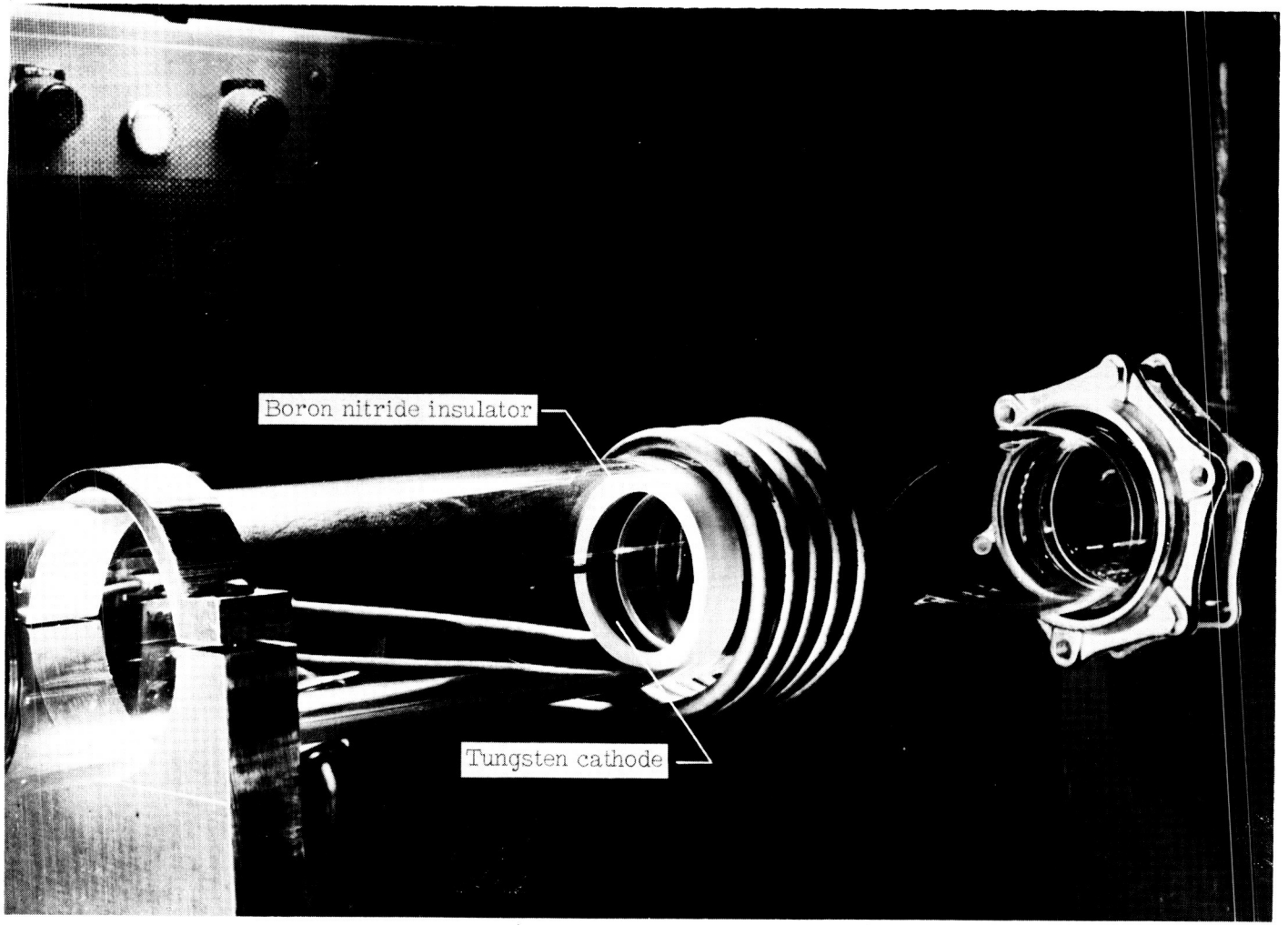

NASA
L-63-4149

Figure 11.- Inductively heated cathode.